



MEKELLE UNIVERSITY

ETHIOPIAN INSTITUTE OF TECHNOLOGY MEKELLE

**SCHOOL OF MECHANICAL AND INDUSTRIAL
ENGINEERING**

Speed Control OF Brushless DC Motor Using Fuzzy controller

A Thesis Submitted to the School of Mechanical and Industrial Engineering of Mekelle University In Partial Fulfillment of the Requirements For the Degree of Masters of Science Mechatronics Engineering.

Advisor : Dr. Durai Prakash

by: Ambasajr Hadush

ID- No: EITM/PR134974/10

Contact address: E-mail: ambasajrames@gmail.com

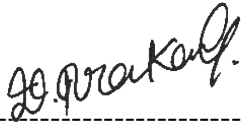
MEKELLE, ETHIOPIA

Thesis Acceptance Approval Form

This is to certify that **Mr. AMBASAJR HADUSH** has incorporated all comments forwarded by the internal and external examiners and the advisor during the thesis defense held on March 24, 2025.

Members of the Examination Board:

Advisor Name: Durai Prakash (PhD)

Signature 


Date 11/09/2025

External Examiner Name: Dr. Kinde Anlay (PhD)

Signature 

Date 11/09/2025

Internal Examiner Name : Dr. Tsegay Tesfay (PhD)

Signature 

Date 11/09/2025

Confirmation: Industrial Automation and Control Chair

Nebyat Gebregziabhier



11/09/2025

Name of the chair Head

signature

date

DECLARATION

I am now ready to announce that the thesis, the work of my original work, is entitled Speed Control of Brushless DC Motors Using Fuzzy Control. The material of this thesis is entirely my own unless the particular references are made. On top of this, the thesis has not been handed in, in full or part, to complete any other academic degree.

BY

Ambasajr Hadush

Approved By;

Advisor Name : D.r Durai Prakash

ABSTRACT

Brushless DC motors are utilized in numerous industrial systems, serving customers, automotive system And applications. Unlike brushed dc motor, brushless motor use electronic commutation and offer several advantage such as compact size, improved performance and high efficient. The existing control method is unable to control speed of a BLDC motor with rapidly changing and uncertain load condition and also could not adapt to load variation with constant gain value. Thus, the main aim of this thesis is to develop a controller to control the motor on the basis of the parameters varying, rated speed and load variations to ensure a fixed output speed of the Brushless DC motor in the presence of different operating conditions. The fuzzy logic controller is an adjustable controller whose development is gradual and progressive towards becoming an efficient control system. In this thesis fuzzy logic has been used to control the speed of the BLDC motor, which offers accurate and precise control. We can validate effectiveness of the proposed method by develop simulation model in MATLAB-Simulink program.

The anticipation of this thesis is that the Fuzzy Logic Controller will outperform PID controller of BLDC motor with respect to settling time (T_s), rise time, and percentage overshoot.

In this thesis, the performance of BLDCM with PID control was analyzed and the results were compared with fuzzy control. The fuzzy controller proved to have a better speed response than PID control.

In a fuzzy intelligent controller, the plant output is varied for obtaining speed control at operating condition. Using MATLAB/Simulink software, MATLAB models and control system simulation were done on the Brushless DC motor. The findings indicate that the intelligent fuzzy controller is better than the traditional PID controller.

Keywords: Fuzzy logic control, PID control, speed control and BLDC motors.

ACKNOWLEDGEMENT

To start, I want to say thank you to My God. I also wish to extend my sincere thanks to my **advisors Dr. Durai Prakash** their assistance, encouragement and even criticism of this thesis. They helped me as much as they could every time I had the chance to present my thesis to them and when I asked questions they always answered in a kind and respectful way, and without their supervision this thesis would not have been possible. I would also like to state that I would like to personally thank all my friends and everyone who helped me complete this thesis successfully.

Table of contents

Thesis Acceptance Approval Form	i
DECLARATION	ii
ABSTRACT.....	iii
ACKNOWLEDGEMENT	iv
LIST OF TABLE	ix
ACRONYMS	x
LIST OF SYMBOLS	xi
CHAPTER ONE	1
INTRODUCTION	1
1.1Background	1
1.2 problem of statement.....	2
1.3Objective	2
1.3.1General Objectives.....	2
1.3.2 Specific Objectives	2
1.4Methodology	2
1.5 Scope and limitation Scope.....	3
1.6Thesis of Organizations	3
CHAPTER TWO	4
LITERATURE REVIEW	4
CHAPTER THEREE.....	6
MATHEMATICAL MODELING AND CHARACTERISTICS	6
3.1Drive modes and structure of brushless DC.....	6
3.1.1Basic structures	6
3.1.2The general design methods of brushless dc motors.....	9
3.1.3 Drive Mode	9
3.2Mathematical Modeling.....	13
3.2.1Differential Equation.....	13
3.2.2Transfer Function (T/F)	22
3.2.3State space Equation (SSE).....	28
3.3.1Steady-State Operations.....	32
CHAPTER FOUR.....	36

CONTROLLER DESIGN OF BRUSHLESS DC MOTORS.....	36
4. PID Controller.....	36
4.3 Fuzzy Logic Controller is employed in this application.	36
4.3.1 Configuration of FLC.....	37
4.3.2Fuzzifier	38
4.3.3 Knowledge Bases	38
4.3.4Decisions making blocks	38
4.3.5 Defuzzifier	38
4.3.6Fuzzy Logic based controllers	39
4.3.7Speed control using fuzzy logic controller.....	40
4.3.8Design methodology of fuzzy logic inferences systems using MATLAB Toolbox	41
4.3.9Select and design MFs	41
4.3.10 Designing membership function for CF.....	42
4.3.11Fuzzy Rule Bases	43
4.4 proposed controller design.....	46
4.4.2 Dynamic BLDC motor specification	47
CHAPTER FIVE	48
RESULTS AND DISCUSSION	48
5.1Responses of system with PID controller	48
5.3System Response no load under Fuzzy Controller	56
5.3System Responses with fuzzy controller under load.....	58
5.3 Numerical Performance Comparison.....	62
5.3.1Numerical Comparison under No load at Rated Speed.....	62
5.3.1Numerical Comparison with load change at rated speed of 1500rpm and 1000rpm.	63
CHAPTER SIX.....	64
CONCLUSION AND FUTURE WORK	64
6.1Conclusion	64
6.2 Future work.....	65
REFERENCES	66
APPENDIX A.....	68
APPENDIX B	70

LIST OF FIGURE

Figure 3.1 Cross-sectional view of motor brushless dc .	7
Figure 3.2 Half-bridge driver circuits [15].	10
Figure 3.3 Full-bridge driver circuits .	11
Figure 3.4 Full-bridge driver circuits of Δ -connected motors.	12
Figure 3.5 C-dump driver circuits .	12
Figure 3.6 H-bridge driver circuits .	13
Figure 3.7 Four-switch driver circuits .	13
Figure 3.8 Structural of the brushless dc motors ...	14
Figure 3.9 types of winding connections...	14
Figure 3.10 Positive direction of provision phaseA..	14
Figure 3.11 permanent magnet flux of phaseA.....	16
Figure 3.12 Effect of rotor saliency on the magnetic circuits[12].....	18
Figure 3.13 Phase relationship between $(\theta), e_A$ and $f_A(\theta)$ [12] .	20
<i>Figure 3.14</i> Brushless dc motor equivalent circuits [12] .	20
<i>Figure 3.15</i> Brushless dc motor equivalent circuit in case when two-phase windings .	23
<i>Figure 3.16</i> Brushless dc motor structure under no load controller system ..	24
<i>Figure 3.17</i> Response curve of brushless dc motors .	25
Figure3.18The speed response process of the system under step inputs [12].	26
<i>Figure3.19</i> Structural systems of brushless dc motor without the armature inductances.....	26
<i>Figure 3.20</i> Speed step response of brushless dc motors without armature inductances[12] ...	27
<i>Figure 3.21</i> structural diagrams of brushless dc motors under load torque .	28
Figure 3.22curve of currents and speed throughout the motor starting process [12] .	31
<i>Figure3.23</i> oscillation and overshoots during the starting process[12] .	31
<i>Figure 3.24</i> Efficiency and armature current curves [12]...	33

Figure3.25 the brushless dc motor characteristics of regulation [12].	34
Figure3.26 the brushless dc motors mechanical properties [12].	35
Figure 4.1 Schematic diagram of atypical fuzzy control systems [12].	37
Figure 4.2 Schematic Representation the architecture of a fuzzy control systems	37
Figure 4.3 Schematic Representation of the CoD max-min inferences[12]	39
Figure 4.4 Schematic Representation of fuzzy control systems	40
Figure 4.5 An Example of triangular-shaped MFs [12]	41
Figure 4.6 Window of the fis editor	44
Figure 4.7 MFS of change and input errors	45
Figure 4.8 MFs of change control output	45
Figure 4.9 Three dimensionally image of control surfaces	45
Figure4.10 Rules Viewer with inputs error, change error and along output (U).	46
Figure 5.1 Simulink model schematic of the PID control systems for the BLDC motor.	48
Figure 5.2 Steps responses of the systems with no load under PID control at 1000 rpm	49
Figure5.3 Step responses of the systems with no load under PID control at 1500 rpm	51
Figure 5.4 Matlab/Simulink model of system with load under PID controller	52
Figure 5.5Step responses of the systems with load under PIDcontroller at 1000 rpm	53
Figure5.6Step responses of the systems with load under PIDcontroller at 1500rpm	55
Figure5.7 Matlab/Simulink model of system with no load under fuzzy controller.	56
Figure5.8 Step response of the systems with no load under fuzzy controller at 1000rpm	57
Figure5.9 Matlab/Simulink model of system with load under fuzzy controller	58
Fig5.10Step response of the systems with load under fuzzy controller at 1000rpm	59
Fig5.11Step response of the systems with load under fuzzy controller at 1500rpm	61

LIST OF TABLE

Table 4.1 Membership function and fuzzy set of input speed errors.....	41
Table 4.2 Membership function and fuzzy set of change input speed error.....	42
Table 4.3 Membership function and fuzzy set of change output control.....	43
Table 4.4 Fuzzy rule base table.....	43
Table 4.5 Brushless dc motor specification [10].....	47
Table 5.1 No-load numerical comparisons of controller characteristics at 1000rpm and 1500rpm.....	62
Table 5.2 Comparison of performance under load variation at 1000rpm and 1500rpm.....	63

ACRONYMS

Permanent magnet brushless dc motor	PMBLDCM
Pulse width modulation	PWM
Permanent magnet synchronous motor	PMSM
High voltage alternative current	HVAC
Digital signal processing	DSP
Proportional-integral derivative	PID
Direct current	DC
Electromagnetic design method	EMDM
Fuzzy logic controller	FLC
Electromotive force	EMF
Field circuit method	FCM

LIST OF SYMBOLS

B_v	Viscous Friction Coefficient
I_x	Phase current
T_e	Electromagnetic torque
T_L	Load torque
u_x	Phase voltage
$e_{\psi x}$	phase-induced EMF
Ω	Angular velocity of rotation
Θ_p	Position angle of rotor
$e_{\psi x}$	Phase induced EMF
Λ_A	Permanence of self-inductance of phase A
Θ	PM flux linkage of phase A
λ_M	Flux linkage
ω_m	Angular speed of the motor
R_x	Phase resistance
L_A	self- inductance of phase A
Θ_A	Angular position of the rotor
R	Resistance of stator per phase
M	Mutual inductance between phase
J	Moment of inertia
N	winding of turns
L	Inductance of stator per phase

CHAPTER ONE

INTRODUCTION

1.1 Background

Two general definitions have been offered by researchers on brushless DC motors (BLDC motors or BLDCMs). One of the perspectives states that only trapezoidal or square-wave back EMF motors can be called BLDC motors, whereas those motors with a sinusoidal EMF at the back can be called permanent magnet synchronous motors (PMSMs) [1, 2]. Other researchers on the other hand view the two types as belonging to the category of BLDC motors [3]. Your new motors run on a DC voltage source to power the motor and the current commutation is done electronically by using a solid-state switching system. The time of commutation depends on the position of the rotor, sensing with position sensor or sensor less techniques. BLDC motors have many advantages including [1]: improved speed-torque performance, high efficiency, high torque –weight ratio, high speed range and extended life span.

As result , the electric vehicles, robotic, HVAC systems, electronic, computers, semiconductor devices, CD-ROMs, medical sector, CNC machine feed drive, and extruder drive are some of the main areas of use of brushless DC motors. These types of application, the motor is often subjected to various forms of load disturbance. The conventional control methods are not often able to provide the required speed regulation and tracking performances in sudden perturbations and change of parameters with steady and accurate precision. To defeat these constraints, more modernized control strategies which include the variable structure controller, fuzzy logic controller, and neural network controller are developed [2].

Brushless DC motor have the commutations electronica carried out by power switch in the inverter circuit. In order to be operated efficiently, the commutation area of the back EMF is to be as small as possible since an even greater area would render commutation of a phase challenging when the current source inverter is driving the motor. Ideally, the flat part of the back EMF is to be 120 degree and this will guarantee a constants torque output. The control system is used as a control mechanism to regulate and control the dynamic behavior of the motor or any other process. Fuzzy control is one of the most used control strategies in the establishment of advanced control systems among other control strategies due to its ability to provide a higher level of performances and precision. With the use of fuzzy logic, the chattering is minimized and the system under control is made stronger.

The (FLC) has been selected as a controller for this thesis due to its several benefits compared to other classical controllers. (FLC) has the merits of its straightforward control design, low cost and can be, unlike an exact mathematical modeling of the system, designed. It is especially efficient to apply in the case of nonlinear systems, including the speed control of DC motors. The thesis focuses on learning the design of FLC that regulate the speed of the (BLDC) motor.

1.2 problem of statement

. Recently, the traditional control systems have not been able to dynamically track closed-loop plant dynamics. Since fix gain controller are used in these systems, they do not work effectively in different condition that include parameters alteration, load variation, and external perturbations. Through this they cannot sustain the desired performance and stability in the process. Today, there is a place for Fuzzy control schemes where traditional control systems are not able to resolve a situation such as:

- ❖ When it comes to performance of specifications of settling Time, rise times and overshoots , there is still a problem.
- ❖ Possibility that frequent or unexpected disturbances, both in and out of control.
- ❖ Loads across the system, inertias or other forces acting on the system can change drastically.

1.3Objective

1.3.1General Objectives

The main aim of the research is to accomplish the design of a fuzzy logic-based control system of the speed control of a (BLDC) motors.

1.3.2 Specific Objectives

- ❖ The mathematically models of brushless dc motors, as well as fuzzy logic algorithm, has been developed.
- ❖ The simulation will use MATLAB/Simulink Module to simulate and design a fuzzy controller.
- ❖ The simulation will be done for two cases. Case 1 will be BLDC with PID control. Case 2 will be BLDC with the Closed loop, Fuzzy controller under with load condition and without load condition.
- ❖ These simulation of pid controls will involve a BLDC Automatically and a response system will be demonstrated using then MATLAB/Simulink software.
- ❖ The controllers is developed to monitor the speed fluctuation as well as to stabilize the motors under varying load.
- ❖ The effectiveness of FLC validated against the PID controller at different rated speed and sudden variations in load.

1.4Methodology

The first task to accomplish the main aim stated above is the evaluation of the literature review of control the speed of bldc motor. Section 1 of this chapter presented a number of existing structures of BLDC motors and drive mode of control. The Typical mathematical model of BLDC motors discussed in detail in the following. To conclude, the stead and dynamics properties of furthermore examined and detailed discussion of transient behavior of torque as

well as current under commutations is provided. The second task is develop a FLC a blank-m file window of editor for the BLDC motor.

The third task is to analyze and discuss the results Simulate the closed-loop model of PID control to demonstrate response obtained from the simulation of the systems utilizing MATLAB/Simulink software and validate of effectiveness the Fuzzy controller operating at different speed compared to PID controller.

Lastly, present the conclusions, suggestions for future research and efforts. In this research we attempted to analyze the speed control of brushless dc motors only on Matlab toolboxes, to concluded that FLC provide better performance and efficiency improvements over PID controllers.

1.5 Scope and limitation Scope

- All models will be simulated using MATLAB/Simulink software.
- We will look at the performance evaluated the parameter such as steady state error settling time, rise time and over shoot and the deviation of speed from desired values when change in reference speeds and load.
- This fuzzy control will be analyzed for different rated speed and load variation.
- The control algorithm will be operate on a personal computer and not on dedicated machine.
- The performance of presented control is not worked practically in the laboratory because of time and practical parameters are unavailability.

1.6Thesis of Organizations

This research is structured as follow. consists of literature Reviews and related studies of brushless dc motors in chapter two. it is primarily mathematical modeling and analysis of the brushless dc motors characteristics is done in chapter three. consist of controller design to control speed a brushless dc motors chapter four. the result and discussion and their analysis are all in chapter five. Conclusion and future work recommendations are in chapter six.

CHAPTER TWO

LITERATURE REVIEW

DC motor are prevalent in various industrials application that require speed and/or position control, such as aerospace, medical device, household appliance, electric vehicle, electric crane, robotic arm, versatility and inexpensive. Furthermore, speeds or positional control of a BLDC motor is also an important topic that continues to be investigated to this day. Various control strategies are introduced the speeds or positional control of a DC motors, with many industrial or high performance applications typically preferring to consider a simple and low cost controller structure. All control theories have advantages, and disadvantages relative to each other, as a result of the respective methods being identified as the preferred control method under specific criteria. This control theory that provides the highest result with particular situation usually the preferred proposed control theory.

Fuzzy logics is also used to regulate the velocity of a BLDC motors in this study. The fuzzy logics was first introduced by Lotfi Zadeh in 1965 and has been used in a wide variety of applications in control systems to artificial intelligences. Through FLC, they are able to use appropriate output parameters.

Also, the idea of a general self-tuning regulators was introduced by Kalman, and it is based on explicit parameter estimation of linearized ,single output and single input systems. The resulting parameters estimation were used to come up with an optimum LQcontrol.

. Scientists have been working towards regulating the speed of an electric motor for to a long time, but only very recently advanced fuzzy logic controllers were developed to address issues arising in electrical and mechanical systems. Control of speed under PWM signals was one of the first strategies developed [1]. The speed and position feedback signals taken at the motor of PMBLDC are used to construct the drive signal of inverter switch. Nonlinear nature of Dc motors, however, like friction and saturation, may have a negative influence on the operation of PID control.

To deal with them, W. Arnold and D. Jacobson (2013) proposes the motor control systems based on neural networks that proves to be highly resilient to structural uncertainties and external disturbances but requires additional computational resources and data storage capacity.

C. Mohankrishna et al (2016) describes a PMBLDC motors state space modeling, simulation and control approach, in which this motors was develop using a state-space model to acquire the state data of the system variables at certain sections of the signal flow. With this mode of modeling, there is no requirement of a high powered processor and a large random access memory., provides more design flexibility, and enables faster results; however, the system still needs an

intelligent controllers adapt to varying load conditions the necessarily reducing speed to prevent the motors from damages.

YI-Yuan Kumar 1,jan2014) and Yee-pien Yang presented title “Angular displacement estimates using Hall-Effect Sensor for Drive a BLPM Motors”. Here they proposed an enhanced techniques for angular displacement estimates using Hall-effect sensor for drive a BLPM motors. Performance of the system is not sufficient, then we need additional control an improve the capacity of the motors.

The thesis , A.M.A Ghany, M.A.A Ghany,”and M.A Shamseldin “Performances Study that Enhanced Non-Linear PID Control Applied on Brushless DC Motor,” International Journal of Drive system (IJPEDS) vol. 9, no.2, pp. 536–545, 2018 and power electronic. Present the findings on better minimizing speed oscillations using a specifically closed loop system understanding the advantage of PID control, [11] especially for tracking system response. The system response is enhanced with fuzzy logic for tracking speed, positioning and speed stabilization tracking. It sets the have better performance and stabilization.

The preceding techniques rely on precise nonlinear model to improve tracking. Several soft compute methods has been many standard feedback control such as PD control , PID control have been introduced to achieving effective speed controls of BLDC motors [3-4]. Nonetheless, one of the significant issues in implementing PID controller for speed and position control system is issues of non-linear for Dc motors[5].

The drawback of being a energy-hungry consumer. The foray into fuzzy logics as a develop philosophy for used the construction of a nonlinear system for embedded control. The architecture can be designed to accommodate non-linearity without resorting to a mathematically models for control development [6]. Fuzzy control methods are utilized for reducing errors by minimizing percentage overshoots to develop systems. Fuzzy control theory reduce steady-state error and percentage overshoot of control systems as well as the capability to remove load disturbances and, as a plus, preserve long motor operating life.

Accordingly, the primary objectives to develop a control systems the guarantee that whatever uncertainties exist of plant parameter and operating condition, errors b/n reference and actual plant outputs is as small as possible.

CHAPTER THREE

MATHEMATICAL MODELING AND CHARACTERISTICS

Brushless dc motors mathematical model of essential the performances assessment and to develop of control systems. In developing the model, we accounted for the structural mode and characteristic operation of brushless dc motors. Typically, brushless dc motors three major part, Include: positional sensing , structure of motors and driving circuits of power. Furthermore, several structural forms of various drive mode. Initial part of chapter three described many exist brushless dc motor structural forms and current driving mode. In this second section, we discussed mathematically common models, mainly the state space models, transfer function, BW models differential equations. Lastly, we analyzed dynamics and steady character and elaborated on varying of torque and currents under commutations.

3.1 Drive modes and structure of brushless DC

3.1.1 Basic structures

The principle behind the construction of a Brushless dc motors is that the mechanical commutator was substituted with an electronic switching circuits. In the traditional DC motors, commutation is performed through the action of brushes under which the magnetic fields is directed in such a way that the armature fields is at right angles with the main field repeatedly. This mechanical commutation process was superseded with electronic technology with the introduction of the inverted dc motors, and physical brushes are no longer necessary. The windings of the armature and the permanent magnets in this arrangement may be mounted on the rotors or stator. An entire brushless DC motors system needs power inverters, control circuitry and rotor position sensors to control the speed of the motor and its direction of rotation .

The brushless dc motors also has a square-waves excitation mode, in contrast to other type of motor, which has a number of benefits, including greater utilisation of PM, reduced size, greater torque, greater efficient and greater reliable . These characteristics help to improve the quality of products, increase their working life, and save a lot of energy. The application of the sophisticated NdFeB permanent magnets also improves the performance and lessens cost and size. A brushless dc motors is structurally similarity to (PMSM) in that it comprises a stators consisting of windings of armature coils, and a rotors consisting of PM. In Figure 3.1, below, the cross-sectional view of a 4 pole brushless dc motors is shown.

3.1.1.1 Stator Core

A Brushless dc motors has the same structural of stator as that of a regular synchronous or induction motors. It is made of a single set or more sets of symmetrical phase winding built into an iron core. The connection of these windings forms a “Y” (star) or a “ Δ ” (delta) connection. The Y connection is more favorable to most applications because it is more cost effective and has superior performances to the X connection since it does not necessitate the use of a neutral

point to connect the winding in a 3-phases on a symmetric connection. In contrast to the conventional brushed dc motors where the windings of armature is mounted on the rotors and serves as the main source of heat, the brushless dc motors mounts its windings of armature on the stators. This design contributes greatly to the reduction of heat generated in the motor making it more efficient and reliable.

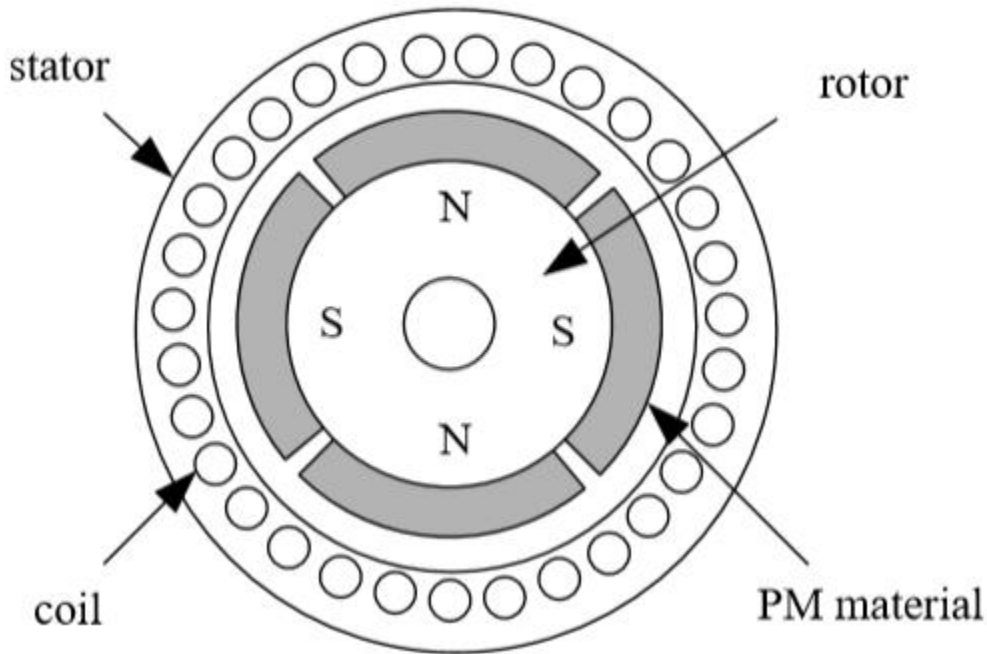


Figure 3.1 Cross-sectional view of motor brushless dc

3.1.1.2 Windings

Various windings that are commonly used in brushless dc motor includes distributed short-pitch windings, distributed full-pitch windings, and concentrated full-pitch windings. The kind of winding chosen has a great influence on back-EMF wave-forms and the performance of motors.

1. The winding is concentrated at full-pitch: In this design, each phase has its wire wound around a single tooth, and this method produces even air-gap flux density over the motors. The sum of all the EMFs of all the phase coils is total back-EMF, which is a reflection of the air-gap flux density shape. As they are the same width, the type of winding creates a very trapezoidal waveform of back EMF that boosts the performance of a motor.

2. Distributed windings; the spread of the windings in the coils can be made throughout the inner part of the stators so as to increase the cooling efficiency. This arrangement is referring to a distribute windings. It is however difficult to obtain a perfect square-waves back-EMF pattern, because of the spatial distribution of the density of the air-gap flux.

3. short-pitch windings contrastingly, short-pitch windings is more economical in uniting the end connection between coils, reduce copper, and reduce torque harmonic. This both makes the winding more material-efficient and also enhances torque smoothness.

3.1.1.3 Rotor of Permanent magnet

. A Brushless dc motors has rotor made of permanent magnetic of particular pole pair, located on the surface of a rotors or within the iron core. Neodymium-Iron-Boron Neodymium material is the most popular; it is a high co-activity re-magnetic material that has very high remanence. These magnets generate a magnetic field medium in air in the gap in a similar manner that they do in the brushed DC motor. Their only major differences however is their placement, the permanent magnet are fixed on the stator in brushed motors whereas they are fixed on the rotor in brushless dc motor.

Common rotor configurations of BLDC motors are three

(1) Surface-mounted Permanent Magnet rotor. In case of Surface-mounted PM rotor, rectangular cross-section rare-earth permanent magnetic tiles are installed radially on the iron core on the outside .They can be assembled through rectangular strips on the pole surface to save costs. Typically, designers tend to use surface-mounted permanent magnet structures with the width of a pole arc commonly picked by the designer may exceed 120° (electrical angle) to obtain nearly square-shaped air-gap flux density which helps avoid torque ripples.

(2) Embedded magnetic rotors: Permanent magnet in this case are incorporated into the rotor iron core. This arrangement improves the concentration of the magnetic flux, because the magnetic flux produced in one pitch of the poles is distributed to the other poles. A non-magnetic (e.g. stainless steel) shaft or magnetic isolation method is commonly used to avoid magnetic interference and maintain structural integrity.

(3) Magnetic loop rotors: Novel, rare earth permanent magnet rings with multi-context pinned radial poles is circumferentially placed round of iron cores. The worth mentioning that this rotor is commonly designed for small power motor.

3.1.1.4 Position Sensors

The angular position of the rotor is sensed by the position sensor on the motor and used to produce electrical signals which provide the logic switching circuits with the requisite commutation information. This makes the current commutated appropriately on the stator winding based on the positional of the rotor and the permanent magnet rotors will keep on rotating. The rotating magnet fields created by the current in the stator through the air gap provides the rotors with movement.

Position sensor can be of different kind , and they have various advantages. Currently, the magnetic, photoelectric and electromagnetic sensor, are more and more common in the brushless dc motor. Of these hall-effect sensors which is a form of magnetic sensors are the most common

because they are small, cheap and easy to use. They, therefore, find wide applications in rotor position detection in BLDC motor control systems.

3.1.2 The general design methods of brushless dc motors

The overall design principles of the brushless dc in motors are FCM and EMDM. The electromagnetic design methods is simpler to use as compared to the finite circuit method, which is more accurate as it allows the magnetic fields to be analyzed in deeper details using the (FEM) and as a result, can be refined on the basis of the simulation outputs. The traditional design approach of design is the EMDM which has four main step:

- a. Set the rotor design according to technicals requirement.
- b. Calculate the magnetic loads (B_0) in relation to arrangement of rotor and the properties of PM.
- c. Calculate an electrical load (A) using (B_{Δ}).
- d. Calculate (A) and (B_{Δ}) compute the fundamental dimensions of the motor (diameter (D) and length (L) using them. Despite being relatively simple and practical EMDM has a lower degree of accuracy.

Finite circuit method , in its turn, is based upon (FEA) of the magnetic fields. In this approach, the parameter of magnetic and electrical circuits are obtained based on the joint analysis of the magnetic field and the electrical circuit. Its key strength is in the capability to generate very accurate magnetic field measurements- two D field analysis is normally enough to satisfy most of the design requirement. Nevertheless, as the magnitude and phase of the equivalent currents can change over time on magnetic field examination, both magnetic and electrical calculations need to be done in parallel so that there is uniformity and precision of the results.

3.1.3 Drive Mode

3.1.3.1 Half-Bridge Modes

A typical 3-phase half-bridge drive circuits of a Y-connection brushless dc motor is a standard 3-phase half-bridge, as illustrated in Figure 3.2. In this arrangement, stator windings of the three phases will be referred to as LA, LB, and LC, phases A, phaseB, and phaseC,. All of the phase windings are connected in series, and each is connected to a separate power switch, T1, T2, and T3. The signals of the rotor positions (HA, HB, and HC) are also amplified to adjust the switching devices to make sure that the motor is commutated properly. In commutation, the stator windings generate a rotating step magnetic field in the air- gaps that is comprised of three separate magnetic states per full electrical rotation of 360 degrees with each state occupying an electrical angle of 120 degrees.

Though the 3 phase half-bridge drive systems has merits like fewer units, cheaper, easily controlled, it has had little adoption because of the limitations inherent in this system; high

torque ripple and poor utilizations the winding since each of the three phases is only energized one-third of the full cycle. Figure 3.2 gives the schematic of this brushless dc motors drive systems.

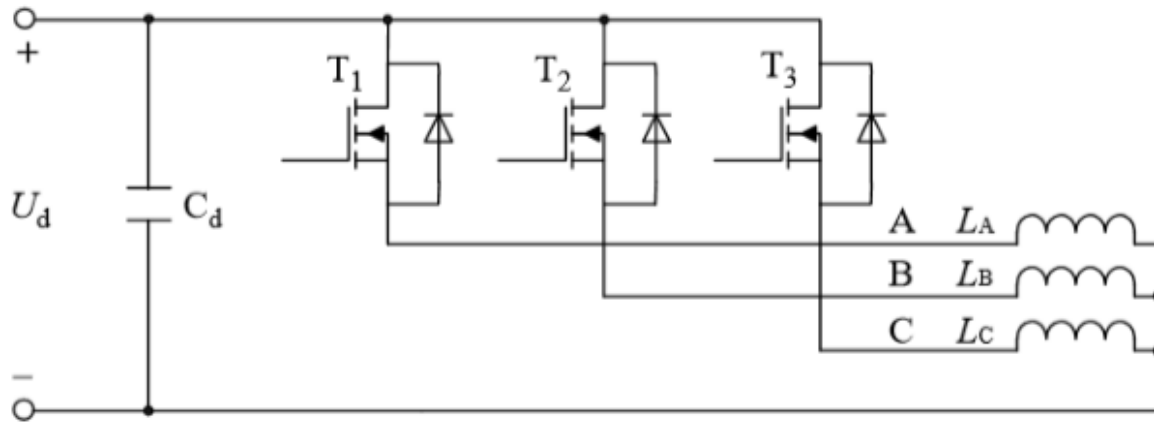


Figure 3.2 Half- bridge driving circuits [12].

3.1.3.2 Full-Bridge modes

A complete bridge driving circuits is shown in the next section based on the example of a 3-phase Y-connection brushless dc motors. Figure 3.3 represents the schematic view of this type of a full-bridge structures. This circuit has been designed with six power switch, T1, T2, T3, T4, T5 and T6 used to regulate the current flowing to the windings on the motor. Logical signal based on the Hall sensor outputs, which are the indication of the rotor position, are used to trigger the switching actions. The drive is usually controlled in either of the following two conduction mode: 2-phase conduction or 3-phase conduction.

A. 2-phase conduction modes:

Two windings of the motor work at any point of this mode with the third winding being inactive. The Hall sensors supply the commutator with the position of the rotor, which it uses to determine the commutation sequence and timing. Consequently, the stator induces the rotating magnetic field which does not change continuously but in discrete steps. The bridge converter performance commutation each time the rotor rotation through 60° the time period for which a current flows continuously in each of the windings is 120° of electric angles. In this interval, the rotor position and magnetic state of the machine is changed. Hence, the current magnetic states of the machine, are 6, each 60° of electrical angle, therefore there are two conducting phase windings in every state. Only one upper bridge switches has beeped at a time in a two phase configuration and the currents may be applied forward through the correspond windings and it will generate torques. Likewise, in a similar manner, torque is also made when the current is in reverse through the winding due to the conduction of a lower bridge switches. The resultant effect of these torques is what is called the synthetic torque. In the given arrangement, the synthetic torque may be

denoted as rotating electrically over a 60 degree angle every commutate cycle. Hence , torque ripples is extremely minimized to a full-bridge drive systems, as the direction of the torque varies six time during a single electrical cycles.

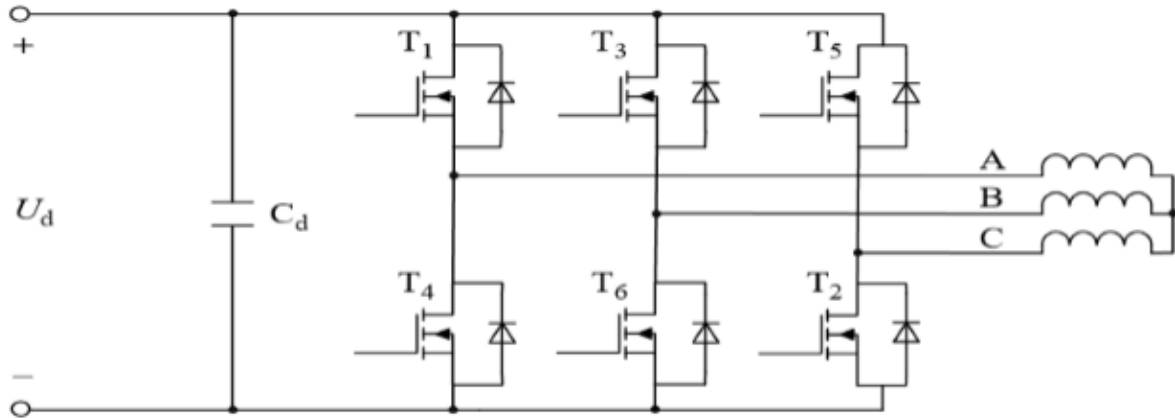


Figure 3.3 Full-bridge drive circuits.

B.3-Phase Conduction Modes:

During the 3-phase conduction modes the 3- power switch of the bridge are always energized at a time. This mode of conduction is the same driving circuits as that of Figure 3.3, therefore, unlike the 2- phase conduction modes. The major differences b/n the two mode is in the series of conduction; in 3- phase conduction the power switches conduction of 180 degrees. This mode gives greater utilization of the winding on the motors and reduced torque ripples. It is however worth marking that in such a set up both the upper switch and lower switch in the arm of the bridge may be conducting concurrently.

The simplistic schematic of a 3-phase full-bridge control systems of a delta -connects 3-phase brushless dc motors is shown in figure 3.4. As shown, the Δ -connected driving circuit has some minor difference with the Y-connected circuit.

3.1.3.3 C-Dump Modes:

The high control performances with small size and inexpensive is one of the requirements in specific brushless dc motors applications. In order to satisfy these requirements Walter and Stephen [13] suggested a compromise between the half-bridge and full-bridge types of control, which became the so-called C -Dump driving circuits. This arrangement is illustrated in Figure 3.5, in which the C-Dump driving circuits is made with a 3-phase brushless dc motors by using only 4- power switch. The design additionally allows 4-quadrant operations the motors as well as minimizes the amount of power switchover as well as the total energy loss, making it an

effective and cost-effective control solution, as compared to the full-bridge operating driving mode. It can lead to larger commutation torque ripples.

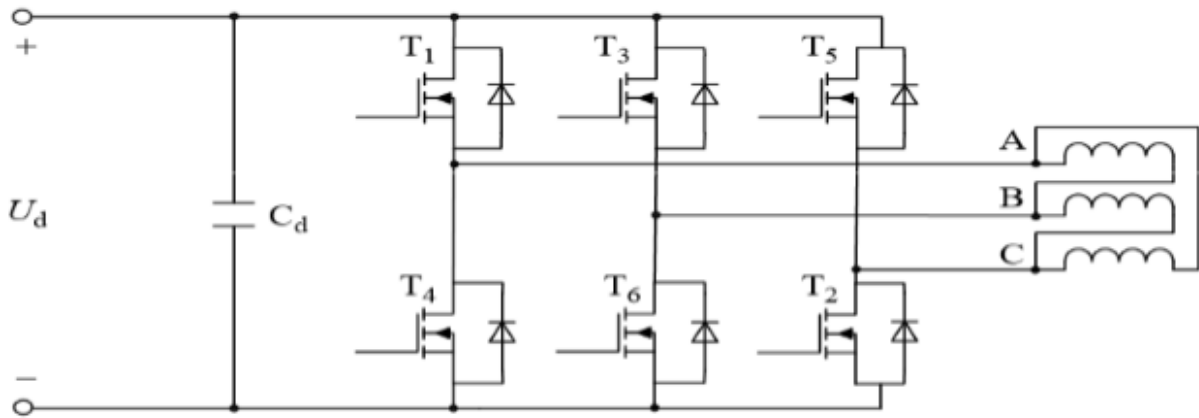


Figure 3.4 Full-bridge driving circuits of Δ -connect motors

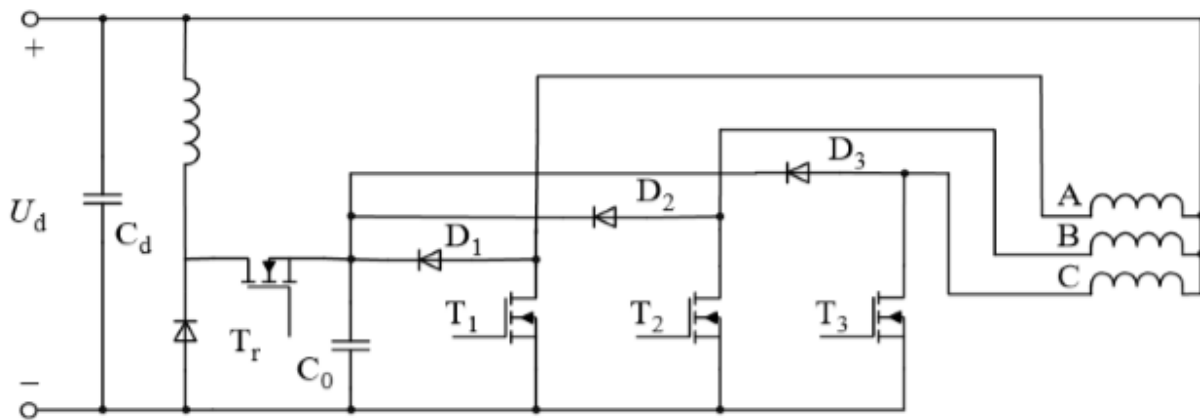


Figure 3.5 C-dump drive circuits.

The H-bridge power inverter is illustrated in Figure 3.6. The H-bridge consists of the distinguishing aspect of each winding being separately control the H-bridge power inverters. driving circuit enables very easy control of the BLDC motor currents. Also, this mode of driving provides four quadrant operation if desired. It is important to note that an H-bridge power inverters uses four power switch to control a single phase windings. Therefore, it is typically employed in one-phase or 2-phase brushless dc motors applications. To prevent simultaneous conduction of the lower switch as well as upper switch in the equal bridge arms, a delay control mechanism must be implemented in the driving signal. This ensures that when one side's switch are turned on, the switch on the opposite side are completely turned off.

3.1.3.4 Four-Switch Mode

The configuration of the four-switch driving circuit is shown in Figure 3.7. In this setup, one bridge of the traditional full-bridge circuits is replaced with 2- capacitors, with the neutrals points between these capacitors connect to the phaseC windings. This modification reduces both cost and power loss in the system; however, it introduces additional complexity in the control algorithm required for proper operation [3].

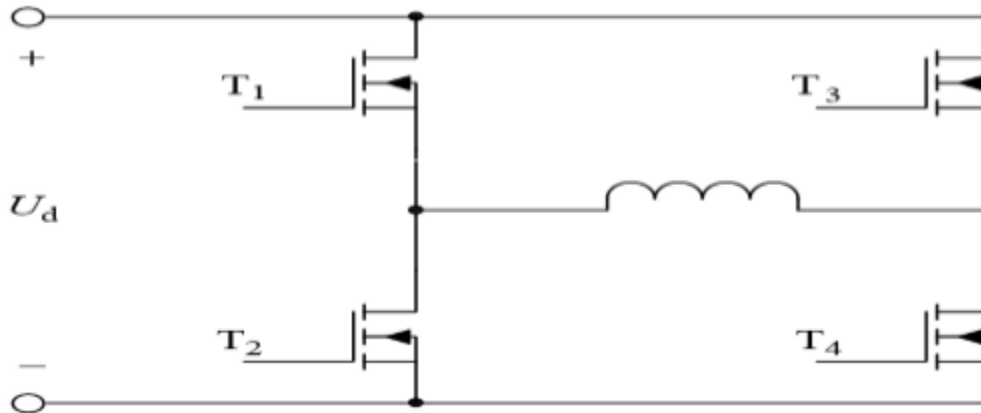


Figure3.6H-bridge circuits.

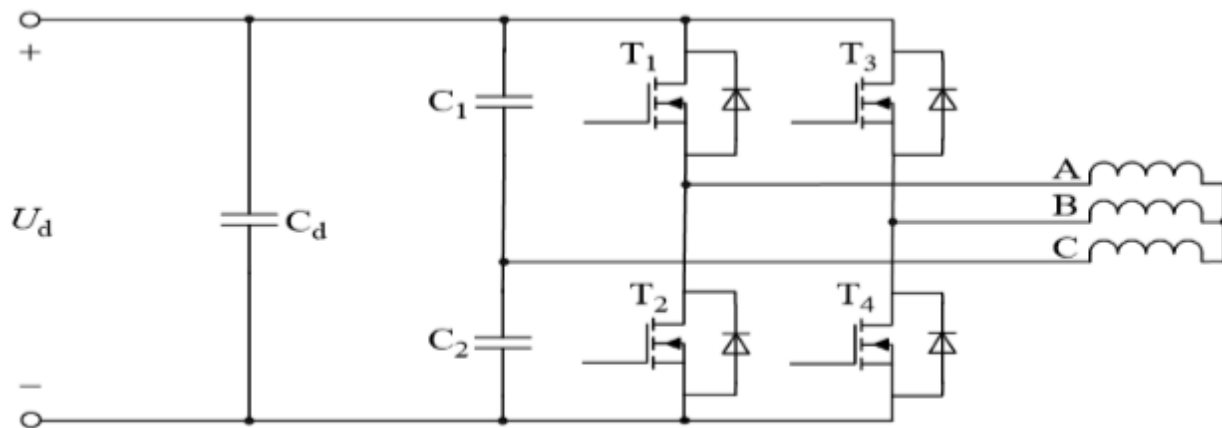


Figure3.7Four-switch drive circuits.

3.2Mathematical Modeling

3.2.1Differential Equation

These part, a 3- phases, 2- poles brushless dc motors is approximated to come up with a (DE) models. This stators is made of full-pitch windings which is linked in Y-arrangement whereas the internal rotors is made without salients poles. The positioning of 3- hall sensor is symmetrical with 120 degrees distance between them. To obtain the differential equation model of the brushless dc motors [14 -15], some simplifying assumption are taken on the controller designs by ignoring some factors as below:

- ✓ Hysteresis loss, eddy currents loss and core loss of the motor are omitted. armature rxn is said to have a trapezoidal waveform.
- ✓ The cogging action is not ignored and the conductor are assumed to be continuously and uniformly distribute over the armature surfaces.
- ✓ Assumptions in the inverter circuits flywheel diode as well as The power switch are assumed to have ideals switch characteristic in the inverter circuits.

So, the simplify analog circuits diagram of the BLDC motor may be presented as follows.

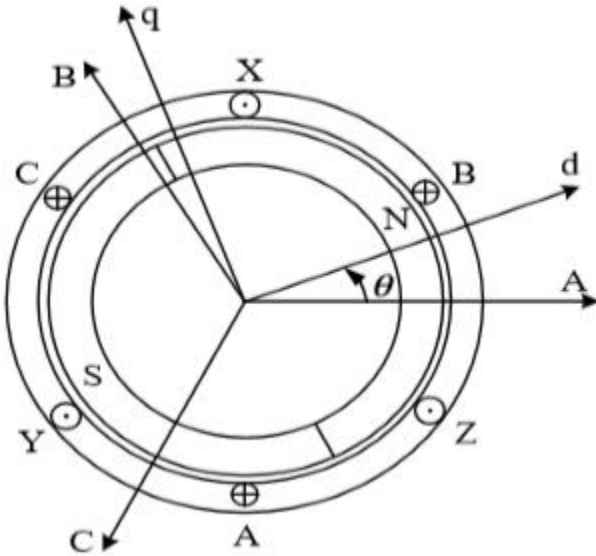


Figure3.8 Structural of brushless DC motors.

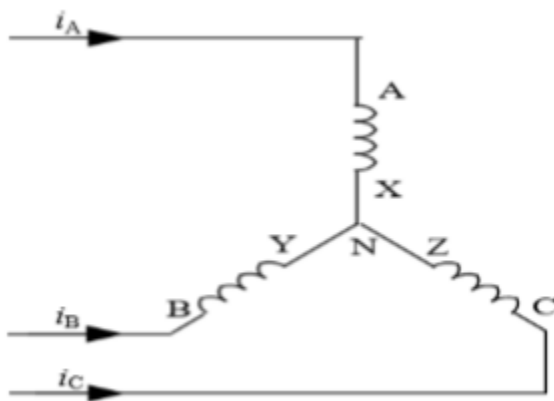


Figure3.9Connected kind of windings.

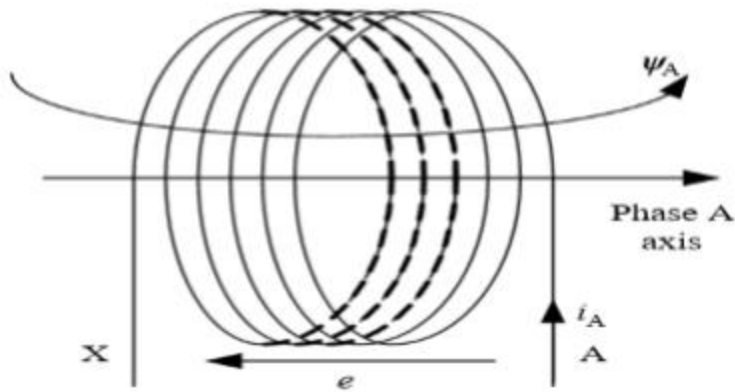


Figure 3.10 Positive direction of provision phase A

Fig 3.10 indicated the positive directions the phase voltage of each stator windings, which consists of the voltage drops across the resistance electromotive force induced represented as:

$$e_{\psi x} + R_x I_x = U_x \quad (3.1)$$

Whereas

x = phase A, phase B and phase C.

R_x - phase resistances.

U_x ----- Phase voltages;

$e_{\psi x}$ ----- Phase electromotive force induced;

I_x ----- Phase currents ;

The resistances are equal phase A, B and C.

Induced EMF because of the winding would be same to the changes of the flux per unit time. Since the EMF and the magnetic flux linkage defined are in the opposite direction to right hand screw rules convention, the electromotive force induce is written as:

$$e_{\psi x} = d_{\psi x} / d_T \quad (3.2)$$

Flux in phase(A) expressed as;

$$\psi_A = L_A i_A + M_{AB} i_B + M_{AC} i_C + (\theta) \quad (3.3)$$

Where ;

M_{AC} ---- mutual inductances of phase A with B, and C.

L_A ---- for phase A Self-inductances;

(θ) ---- for phase A permanent magnet flux linkages.

Size of (θ) is function of the permanent magnet air gap distribution. The magnetic field's radial component due to the PM distribute as a trapezoidal profiles on the internal layer of the stators show below in Fig 3.11.

If the rotors rotate in the direction of anticlockwise the Ax moved in the directions of forward on the axis of y as shown in fig 3.11. The effective phase A flux will vary accordingly based on the rotor positions. At rotor positions the permanent magnet flux of phaseA can be expressed as,

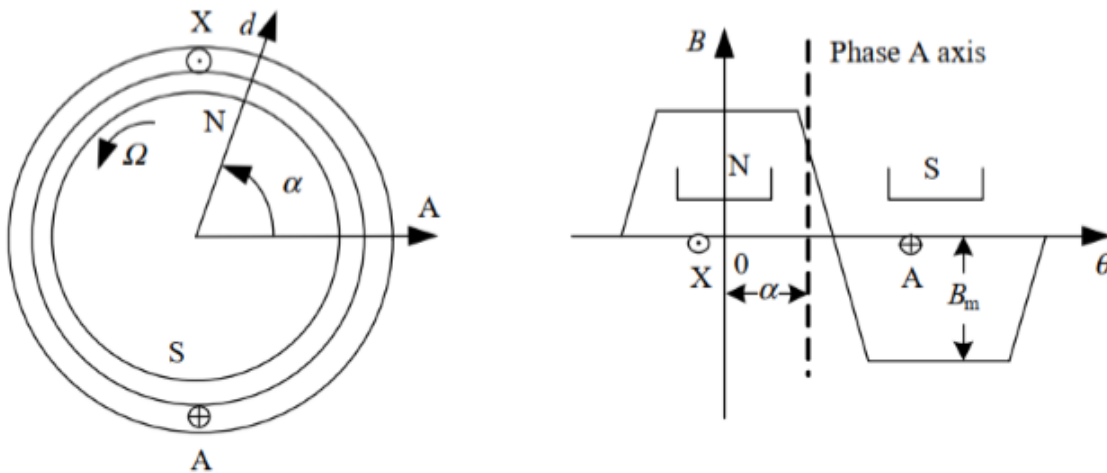
$$\lambda(\alpha) = \lambda(\alpha) \quad (3.4)$$

$$\lambda(\alpha) = \int_{-\frac{\pi}{2}+\alpha}^{\frac{\pi}{2}+\alpha} B(\theta) S d\theta \quad (3.5)$$

Whereas

$\lambda(\alpha)$ ---- permanent magnet flux for phaseA

$B(\theta)$ ---- represents the radial flux density of the permanent magnet rotors with in air gaps ,exhibiting trapezoidal distributions along the y axis;



(a) positions of rotor

(b) distributions of flux

Figure 3.11 permanent magnet flux for phase A.

S - effect length for conductor and products of rotors radius .

N .. Turn of windings;

Equation (3.2)-(3.5) substitute into equations (3.1), then :-

$$\begin{aligned}
 u_A &= Ri_A + \frac{d}{dt} (L_{Ai}i_A + M_{AB}i_B + M_{AC}i_C \psi_{pm}) \\
 &= Ri_A + \frac{d}{dt} (L_{Ai}i_A + M_{AB}i_B + M_{AC}i_C) + \frac{d}{dt} [NS \int_{-\frac{\pi}{2}+\theta}^{\frac{\pi}{2}+\theta} B(x)dx] \\
 &= d/dt (L_{Ai}i_A + M_{AB}i_B + M_{AC}i_C) + e_A + Ri_A
 \end{aligned} \tag{3.6}$$

Whereas e_A denotes the electromotive force for phase A. derivative operation in equation (3.6) refers to the products the current and inductance, where mutual inductances and self-inductance of windings depend on N^2 and the permanent of the associated magnetic circuits.

This:

$$L_A = N^2 \Lambda_A \tag{3.7}$$

$$M_{AB} = N^2 \Lambda_{AB} \tag{3.8}$$

Whereas

Λ_{AB} ---- Permanence of mutual inductances flux b/n phase A and B.

Λ_A --- Permanence self-inductances flux of phase A.

There is a variation in the permeability of salient poles rotors along the q-axis and d-axis, leading to variation in mutual inductance as well as self-inductance of winding with position of rotors. [16]. So, the inductance depend on the rotor positions. In contrast for non-salient rotors magnetic flux is uniform all directions and the permeability of the magnetic circuits, to be affect by rotor positions. Therefore, for the case of a rotor with no saliency, the mutual and self-inductance cannot change in time. Fig 3.12 illustrates the saliency effect of the rotor on winding inductances.

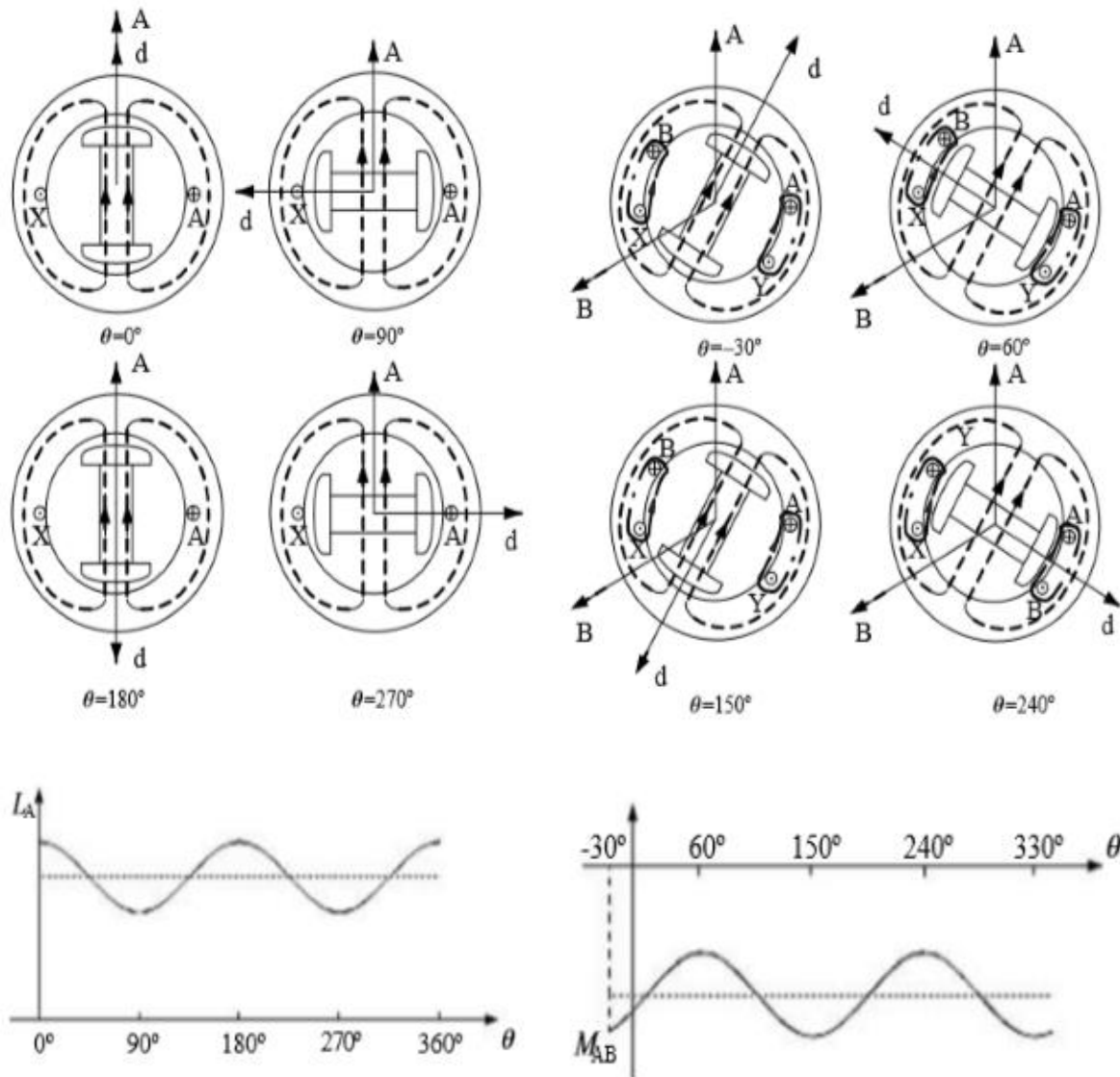


Figure 3.12 Effect of rotor saliency on the magnetic circuits [12]

Typically, for surface-mounted non-salient-poles rotors used in brushless dc motor. Here, the windings inductances do not vary with rotor positions. Furthermore, since 3-phase stator windings are symmetrical, each has the same self-inductance and each pair of phases has the same mutual inductance. This is $M_{AB} = M_{BC} = M_{CA} = M$ and $L_A = L_B = L_C = L$. Substitute into the Equations (3.6), hence we set;

$$u_A = R i_A + L \frac{di_A}{dt} + M \frac{di_B}{dt} + M \frac{di_C}{dt} + e_A \quad (3.9)$$

In which,

$$\begin{aligned}
e_A &= d/dt \left[\int_{-\frac{\pi}{2}+\theta}^{\frac{\pi}{2}+\theta} B(x) dx \right] \\
&= \left[-(-\pi/2 + \theta) / dt + (\pi/2 + \theta) \right] \\
&= \left[-(-\pi/2 + \theta) + (\pi/2 + \theta) \right] \qquad \qquad \qquad 3.10
\end{aligned}$$

Where ω is the brushless dc motors angular speed.

Based on magnetic density distributions in the air gaps as illustrated in fig 9, and considering that $B(\Theta)$ has period of 2π and $(B(\Theta+\pi)=-B(\Theta))$, expressed as:

$$\begin{aligned}
e_A &= \left[-(-\pi/2 + \theta) + (\pi/2 + \theta) \right] \\
e_A &= \left[(\pi/2 + \theta) - (-\pi/2 + \theta + \pi - 2\pi) \right] \\
e_A &= 2(\pi/2 + \theta) \qquad \qquad \qquad 3.11
\end{aligned}$$

so, the electromotive force waveform phaseA which change with Θ lead the air gaps magnetic density distributions by $\pi/2$.we can get :

$$e_A = 2(\Theta) = (\Theta) \qquad \qquad \qquad (3.12)$$

It is noted that (θ) exhibits a trapezoidal distributions with respect rotor positions, where its minimum and maximum value are negative one and positive one respectively, and the correspond wave as well as it phases reference with (θ) and e_A are presented in Figure 3.13, also for the 3-phases symmetrical winding there are exists, $f_A(\Theta) = f_A(\Theta - 2\pi/3)$ as well as $f_C(\Theta) = f_A(\Theta + 2\pi/3)$.

from equation (3.10) it is evident that e_A represents a rotates back electromotive force generated by the windings flux resulting from the rotation motor.

3-phase satisfy;

$$I_A + I_B + I_C = 0 \qquad \qquad \qquad (3.13)$$

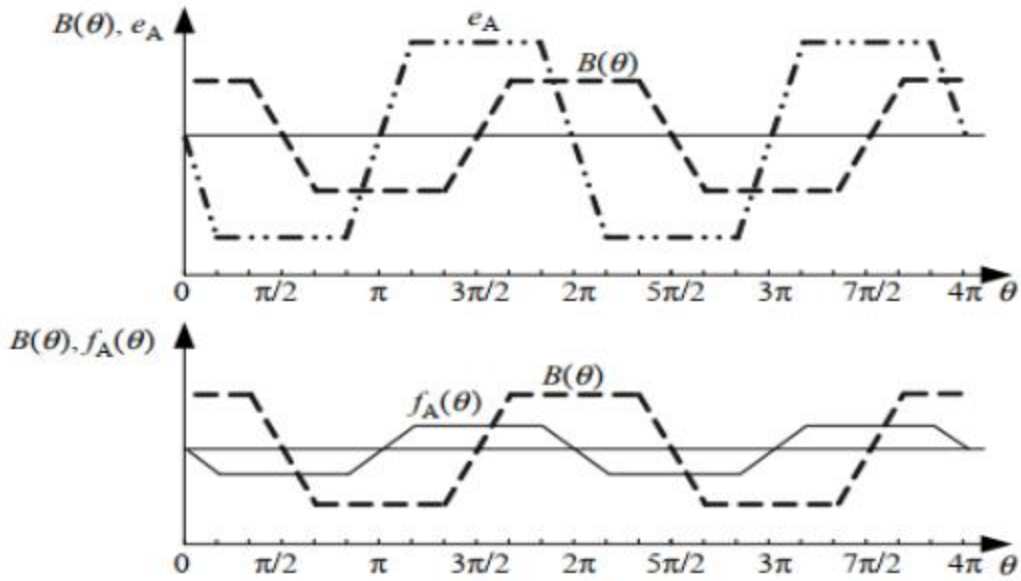


Figure 3.13 Phases relationship between $(\Theta), e_A$ as well as $f_A(\Theta)$ [12].

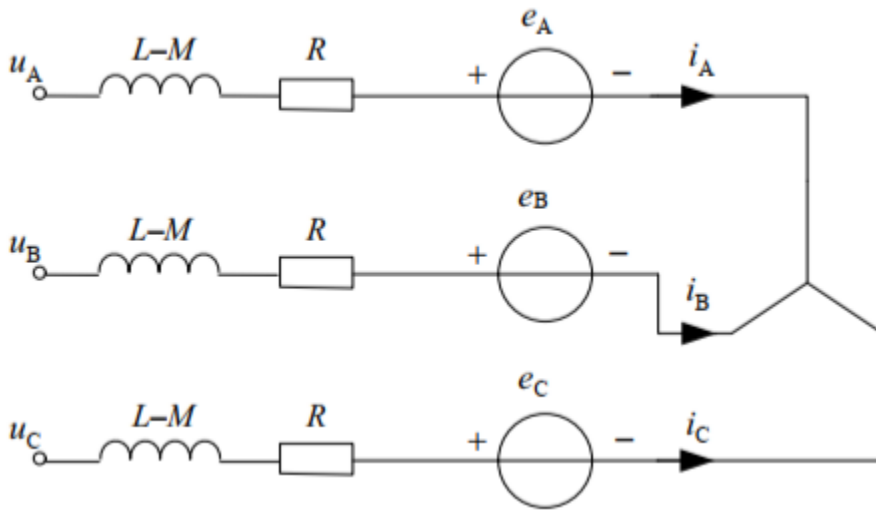


Figure 3.14 Equivalent circuits of the brushless dc motors [12].

simplify Equations (3.9)

$$(l-m) \frac{di_A}{dt} + e_A + Ri_A = U_A \quad (3.14)$$

brushless dc motors phase voltage equations in matrix represent as:

$$\begin{bmatrix} u_A \\ u_B \\ u_C \end{bmatrix} = \begin{bmatrix} R & 0 & 0 \\ 0 & R & 0 \\ 0 & 0 & R \end{bmatrix} \begin{bmatrix} i_A \\ i_B \\ i_C \end{bmatrix} + \begin{bmatrix} l-m & 0 & 0 \\ 0 & l-m & 0 \\ 0 & 0 & l-m \end{bmatrix} \frac{d}{dt} \begin{bmatrix} i_A \\ i_B \\ i_C \end{bmatrix} + \begin{bmatrix} e_A \\ e_B \\ e_C \end{bmatrix} \quad (3.15)$$

As indicated by equations (3.15), equivalent circuits for brushless dc motors can be represented in Fig3.14. In the case of the brushless dc motor pertaining to most applications, the stators winding are Y- connection and do not bring out a neutral point so that phases voltage are not easy to detects. The mathematical models using phase voltages applies to some cases, but not all. The line voltage, is easier to measures, and when appropriate power transistors are in the on state, the line voltages will be approximate the same to dc bus voltages (again, with some exceptions). So, it follows that the mathematical models using line voltages will work better for depiction of the practical's systems.

Equations of the line voltages can obtain from the subtracting determine the equations of phase voltages;

$$\begin{bmatrix} u_{AB} \\ u_{BC} \\ u_{CA} \end{bmatrix} = \begin{bmatrix} R & -R & 0 \\ 0 & R & -R \\ -R & 0 & R \end{bmatrix} \begin{bmatrix} i_A \\ i_B \\ i_C \end{bmatrix} + \begin{bmatrix} l-m & m-l & 0 \\ 0 & l-m & m-l \\ m-l & 0 & l-m \end{bmatrix} \frac{d}{dT} \begin{bmatrix} i_A \\ i_B \\ i_C \end{bmatrix} + \begin{bmatrix} e_A - e_B \\ i_B - e_C \\ i_C - e_A \end{bmatrix} \quad (3.16)$$

These torque and power analysis of brushless dc motors can be performed from an energy transfers point of view, similar to the case of DC motors. When the motors is in operation, power from the supply, and some power is converted to iron loss as well as copper loss, the majority of the power is transmitted across air gaps and to the rotors in the form of mechanical torque effects. The power transferred to the rotor, or electromagnetic power, is equal to the sum of monetary of currents times the back electromotive force of 3- phase. Namely,

$$pe = e_A i_A + e_B i_B + e_C i_C \quad (3.17)$$

Ignoring electromagnetic power, mechanically loss and the stray loss is total turns into KE ;

$$pe = T_e \Omega \quad (3.18)$$

Where ; T_e ----- Electromagnetic torques;

Ω ----- Angular velocity rotational.

Therefore , by combining Equation (3.18) and (3.17), that obtain;

$$T_e = \frac{e_A i_A + e_B i_B + e_C i_C}{\Omega} \quad 3.19$$

Substituted Equations (3.12) to Equations (3.19) the torque expressed as;

$$T_e = [\psi(\theta) i_B + \psi m f C(\theta) i_C + (\theta) i_A] \quad (3.20)$$

When the BLDC motor operates with 1200 commutation and we neglect the the current that have the same amplitude, transients commutation process, and oppositional dxn will flow through the 2-phase winding of the Y-connection motors at any instant. We observe that the signs of (θ) at the flat-top regions oppositional for corresponding windings. Consequently the equation (3.20) simplify :

$$T_e = 2p \psi_m i_A = K_T i \quad (3.21)$$

Where

K_T ----- coefficients torque;

i ----- phase currents at steady. Mathematically models of the electro mechanical systems;

$$T_e - T_L = J \frac{d\Omega}{dt} + B_V \Omega \quad (3.22)$$

Wheres; T_L ----- loadtorques;

J ----- Rotors ofmoment of inertia;

B_V ----- Viscousfriction coefficients.

3.2.2 Transfer Function (T/F)

The T/F is the main concepts of control theory that is a key to the modeling, analysis, and design of automatic control systems. Most classical control designs and analysis techniques, including frequency-response methods and the root-locus methods are constructed by use of the transfer function method.

The T/F is very important in performances evaluation and placement of suitable control strategies in the case of a brushless dc motors. The stator windings of the brushless dc motors has energize depending on the positions of the rotors, usually in multi-phases or 3- phase format as opposed to a conventional brushed dc motors. However, the basic rules of operation of back-electromotive force generation and EMT generation are similar to the brushed dc motors.

As an example, consider a 3-phases brushless dc motors being powered by a full-bridge inverters working in 2-phase conductions modes, at any point in time, when phases A and B are connected to the load, the state of the system might be described in the following way:

$$\left\{ \begin{array}{l} i_A = i_B = i \\ \frac{di_A}{dt} = \frac{di_B}{dt} = \frac{di}{dt} \end{array} \right\} \quad (3.23)$$

equations(2.16) voltage line we get;

$$U_{AB} = 2(1-m) \frac{di}{dt} + (e_A - e_B) + 2Ri = U_{AB} \quad (3.24)$$

When transient process neglected (that is, trapezoid level edge not consider), the steady e_A and e_B are same in amplitudes, but opposite in directions, we turn on phase A and phases B. Consequently, Equation (3.24) written as:

$$2(L-M)\frac{di}{dt} + 2e_A + 2Ri = U_{AB} = U_d = L_a \frac{di}{dt} + K_e \Omega + r_a i \quad (3.25)$$

U_d ----- bus dc voltages;

r_a -----Line resistances of windings, $2R=r_a$;

L_a ----- Equivalent line inductances of windings $2(-M+L)=L_a$

K_e ----- coefficients of the line back electromotive force, $4pNsBm = K_e = 2p\psi m$, Equations (3.25) is precisely the armature voltages loop equations when exciting 2- phases winding, and the equivalent circuits is presented in Figure 3.15. It is important equivalent circuits presented in Figure 3.15 could be applied in 3-phases full-bridge driving mode and 3-phases half bridge driving of the brushless dc motors, with the proper K_T and K_e specifications.

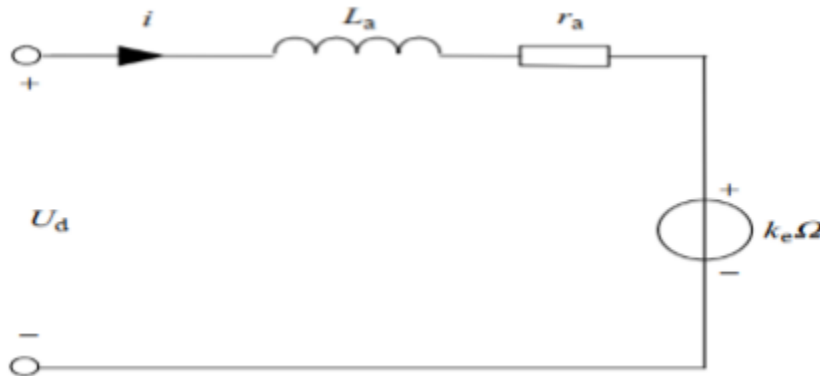


Figure 3.15 Brushless dc motors equivalent circuits in case when two-phase windings

The Equations (3.25), if the currents can be represented in terms of angular velocity, so, transfer function of a motor can be obtained through a relationship between bus voltages and angular velocity. Next, we substitute equations (3.21) to equations (3.22) to obtain:

$$K_T i - T_L = J \frac{d\Omega}{dt} + B_V \Omega \quad (3.26)$$

At start, if the brushless dc motors run under no loads, currents will be;

$$\frac{B_V \Omega}{K_T} + \frac{J}{K_T} \frac{d\Omega}{dt} = i \quad (3.27)$$

Substitute equations (3.27) into Equations (3.25), given as;

$$U_d = r_a \left(\frac{J}{K_T} \frac{d\Omega}{dt} + \frac{B_V}{K_T} \Omega \right) + \frac{d}{dt} \left(\frac{J}{K_T} \frac{d\Omega}{dt} + \frac{B_V}{K_T} \Omega \right) + K_e \Omega \quad (3.28)$$

Also, it can be rearranged as:

$$U_d = \frac{KTd2\Omega}{dt^2 + r_aJ + L_aBV} + \frac{KTd\Omega}{dt + r_aBV + k_eKT} + \frac{KT\Omega}{KT} \quad (3.29)$$

$$U_d = \frac{L_aJ}{KT} \frac{d^2\Omega}{dt^2} + \frac{r_aJ + L_aBV}{KT} \frac{d\Omega}{dt} + \frac{r_aBV + k_eKT}{KT} \Omega \quad (3.29)$$

The BLDC motor transfer function using Laplace transformation equation (3.29) as follows;

$$G_U(s) = \frac{\Omega(s)}{U_d(s)} = \frac{KT}{L_aJS^2 + (r_aJ + L_aBV)S + (r_aBV + K_eKT)} \quad (3.30)$$

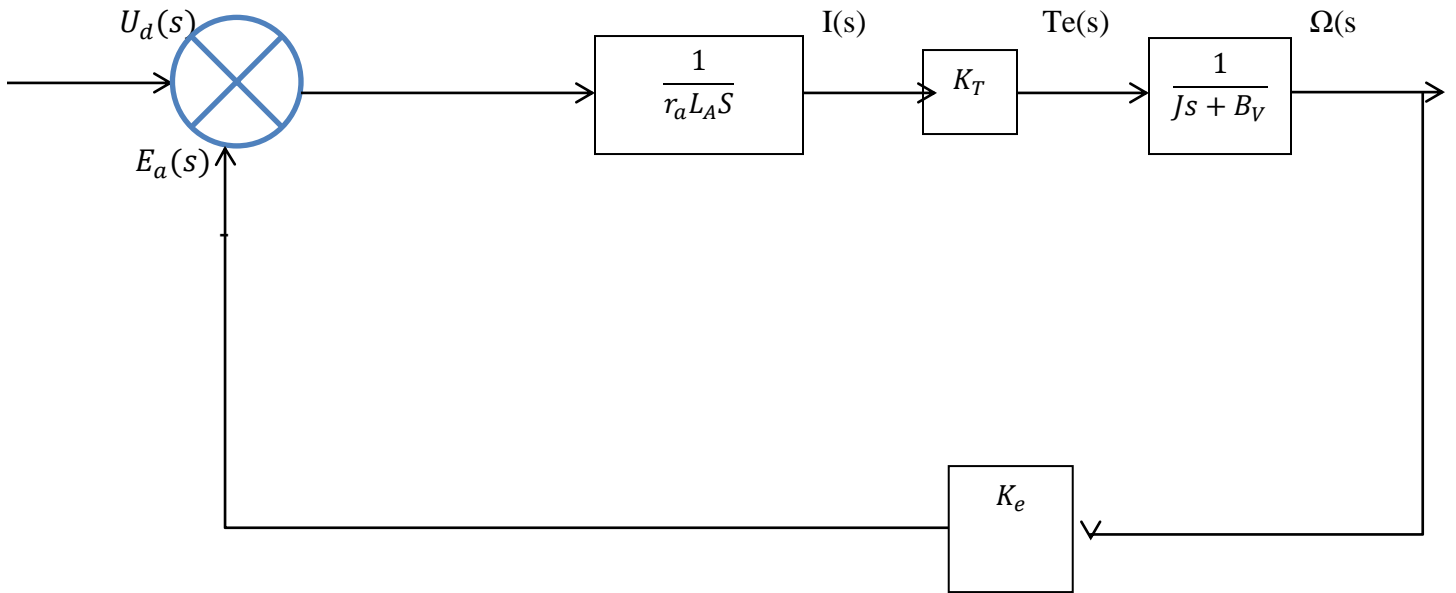


Figure 3.16 Brushless dc motor structure under no load controller systems ..

The second order system of equation (3.30) the BLDC motor implies that;

$$G_U(s) = \frac{KT}{r_aBV + K_eKT} \frac{\omega_n^2}{(S^2 + 2\xi\omega_nS + \omega_n^2)} \quad (3.31)$$

Where;

$$\omega_n = \sqrt{\frac{r_aBV + K_eKT}{L_aJ}} \quad \text{-----} \quad 2^{\text{nd}} \text{-order natural frequency of systems}$$

$$\xi = \frac{1}{2} \frac{r_aJ + L_aBV}{\sqrt{L_aJ} \sqrt{r_aBV + K_eKT}} \quad \text{-----} \quad 2^{\text{nd}} \text{-order damping ratio systems.}$$

As can be seen in relation to the Equations (3.31) the 2nd- root of characteristics equations of the 2nd-order systems of brushless dc motors represents as $S_{1,2} = -\xi\omega_n \pm \omega_n\sqrt{\xi^2 - 1}$ the

response time of the systems is imposed by both ξ and ω_n . In case of a unit step inputs, the convergence speed of the response curves is dictated by ω_n . A larger ω_n correlates with generally faster convergence speed. Additionally, ξ that dictate the characterize of eigenvalue and general form of response curves. The systems operates at over damped, under damped and critically damped. When $\xi > 1$, $0 < \xi < 1$ and $\xi = 1$ respectively. The response curve rate of these differences is in Figure 3.17.

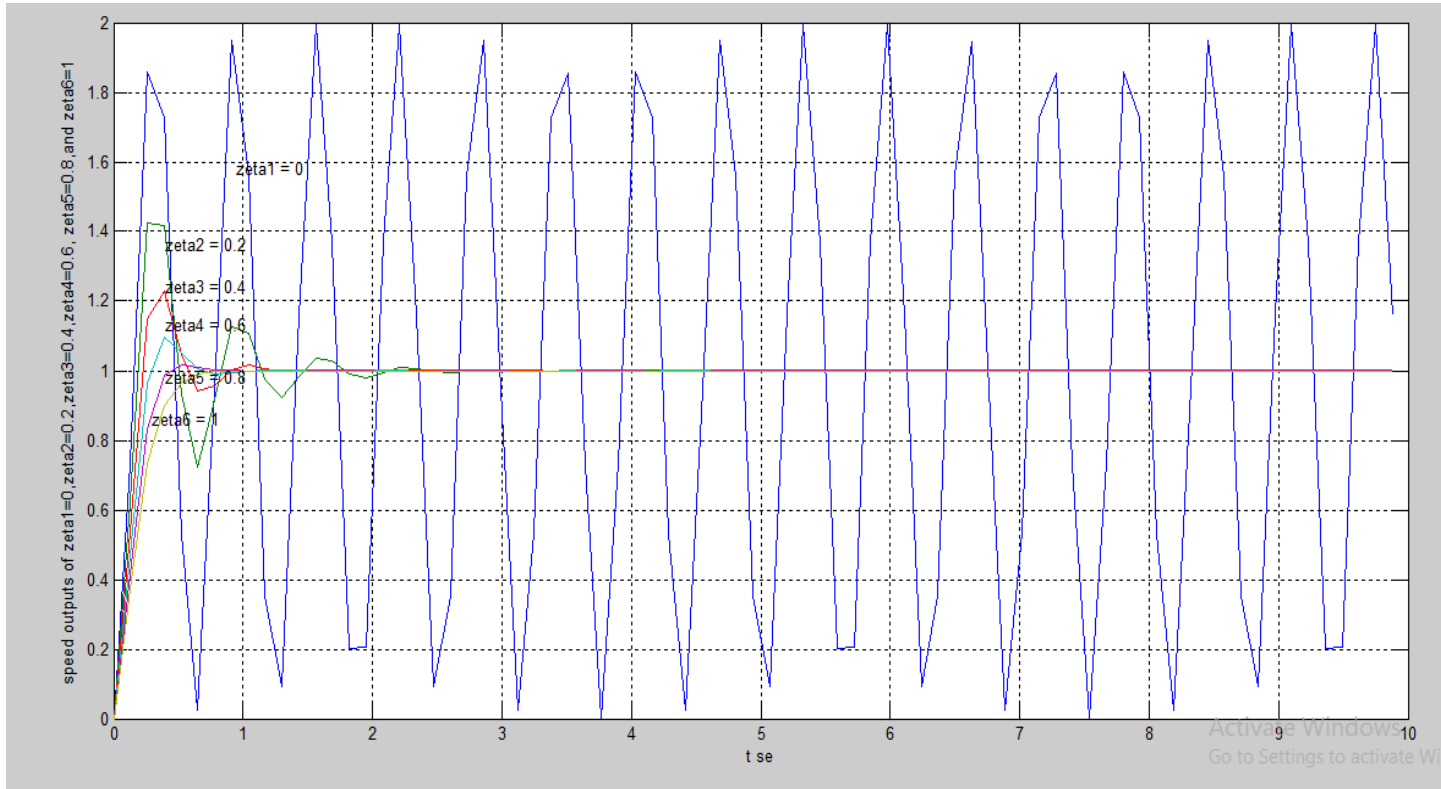


Fig3.17 Response curve of brushless dc motors.

Assume mechanically time $t_m = \frac{r_a J + L_a B_V}{r_a B_V + K_e K_T}$

$T_e = \frac{L_a J}{r_a J + L_a B_V}$ The equation (3.30) can be;

$$G_U(s) = \frac{K_T}{r_a B_V + K_e K_T} \frac{1}{(S^2 t_m t_e + S t_m + 1)} \quad (3.32)$$

Generally, mechanically time constant is very large compared to the electromagnetics time constant. Thus, one can simplify Equation (3.32) to get the transfer function:

$$G_U(s) = \frac{K_T}{r_a B_V + K_e K_T} \frac{1}{S^2 t_m t_e + S t_m + 1}$$

$$G_u(s) = \frac{K_T}{r_a B_v + K_e K_T} \frac{1}{(s t_m + 1)(s t_e + 1)} \quad (3.33)$$

It is apparent, based on Equations (3.33), the T/F of brushless dc motors represented in 2-inertia component, connected in series. Fig3.18 [17] shows the corresponds response of the speed to a step inputs. The value of this figure can also be used to interpret the physical meaning of the time constants in the T/F. On application of a step voltages at the input the first response is found in the currents following a reaction to the changes of the voltages via the $(1/(s t_e + 1))$, where (t_e) is the electrical time constants. The motor speed is then reacted to the current changes by the $(1/(s t_m + 1))$ connection, (t_m) is the equivalent mechanical time constants. Fig3.19 shows the dependence between the angular speed and the armature currents.

If we neglect the influence of electromagnetic time constants, which means that armature inductance can be considered negligible, L_m can be regarded as zero, hence Equation (3.32) can now be stated in simpler terms the 1st order models expressed as follows;

$$G_u(s) = \frac{K_T}{r_a B_v + K_e K_T} \frac{1}{s t_m + 1} \quad (3.34)$$

from equations (3.34) in step response expressed as;

$$\Omega(t) = \frac{K_T U_d}{r_a B_v + K_e K_T} \left(1 - e^{-\frac{t}{t_m}} \right) \quad (3.35)$$

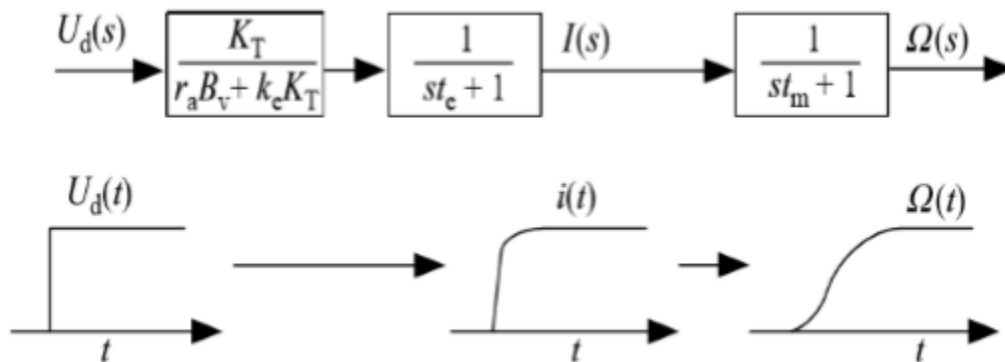


Figure3.18The speed response process of the system under step inputs [12].

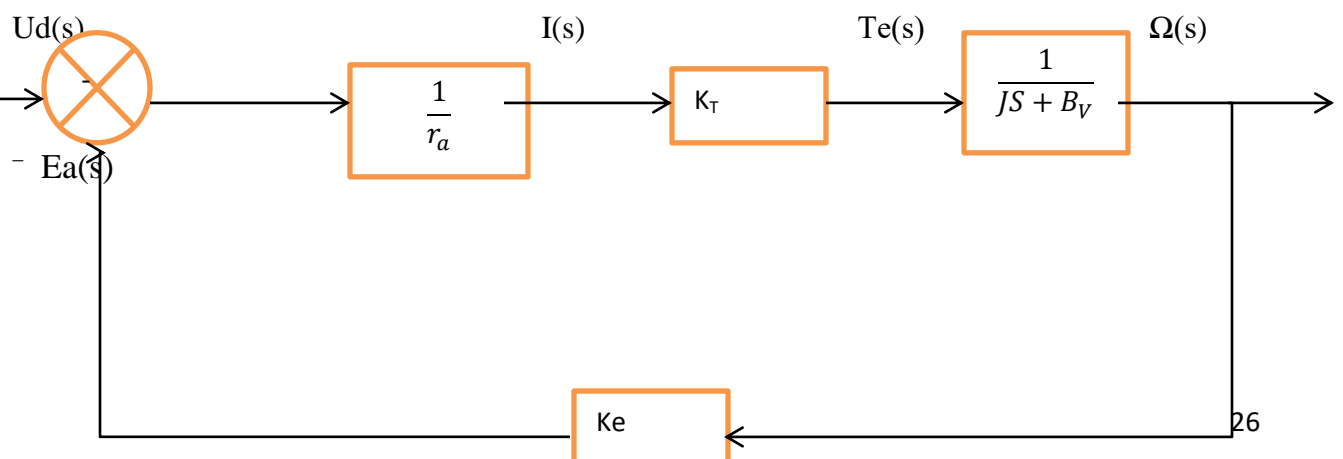


Figure3.19 Structural systems of brushless dc motors without the armature inductances

Figure3.20 depicts that the mechanical time constants (t_m) decrease, the settling time of speed response becomes short. In speed control systems, it is desired to have a small enough delay time for speed response. If the (t_m) constants is large, we should design a proper closed control system to increasing the speed of response. For instance, we can use either a currents or voltages amplifier with a high gains in an analog control systems. On the other hand, too large of a gain would in turn cause larger losses of power switches which would decrease systems efficiency. Additionally, from a controls perspective, a high proportional gains may induce instability and oscillation.

Thus, in the system design, the speed response as well as the stability of the system must be treated together. The speed response can be increased within stability constraints.

In the next step, it will be discussed that a BLDC motor is tested with a positive value for the load torque. With this condition, the load torques of the BLDC motors can be considered as an inputs load variation for systems, as evidenced in Figure3.21.

In a system like that the superposition's principles hold, the system outputs is equal to the outputs when (s) is applied to the system calculations or (s) is applied to the system calculations. When assuming (s) = 0 as shown in Figure 21, therefore,

$$\Omega(s) = \frac{1}{Js+B_V} \left[-K_e \frac{1}{r_a+L_a s} K_T \Omega(s) - T_L(s) \right] \quad (3.36)$$

$$T_L(s) = -\Omega(s) \left[\frac{(r_a+L_a(s)(Js+B_V)+K_e K_T}{(r_a+L_a s)} \right] \quad (3.37)$$

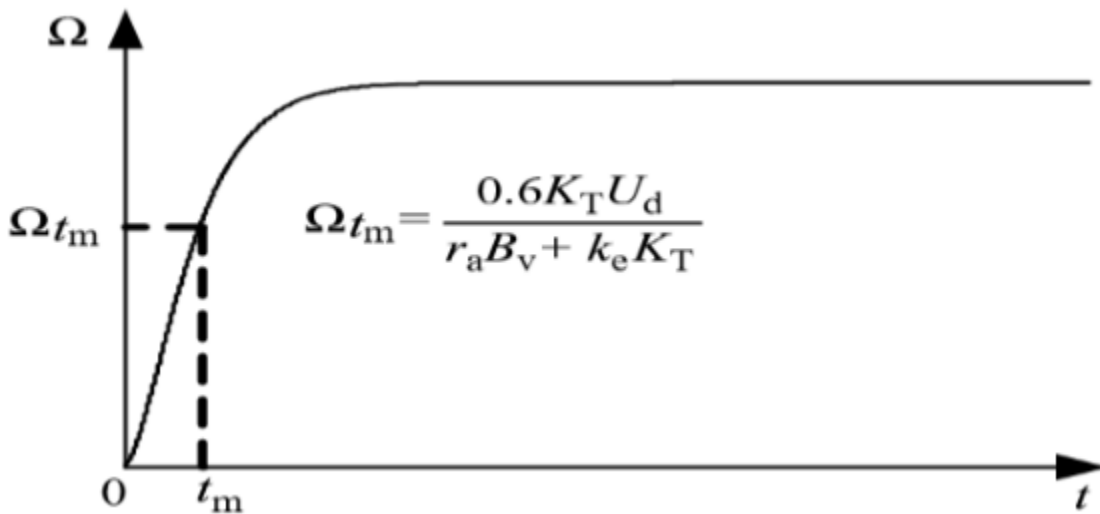
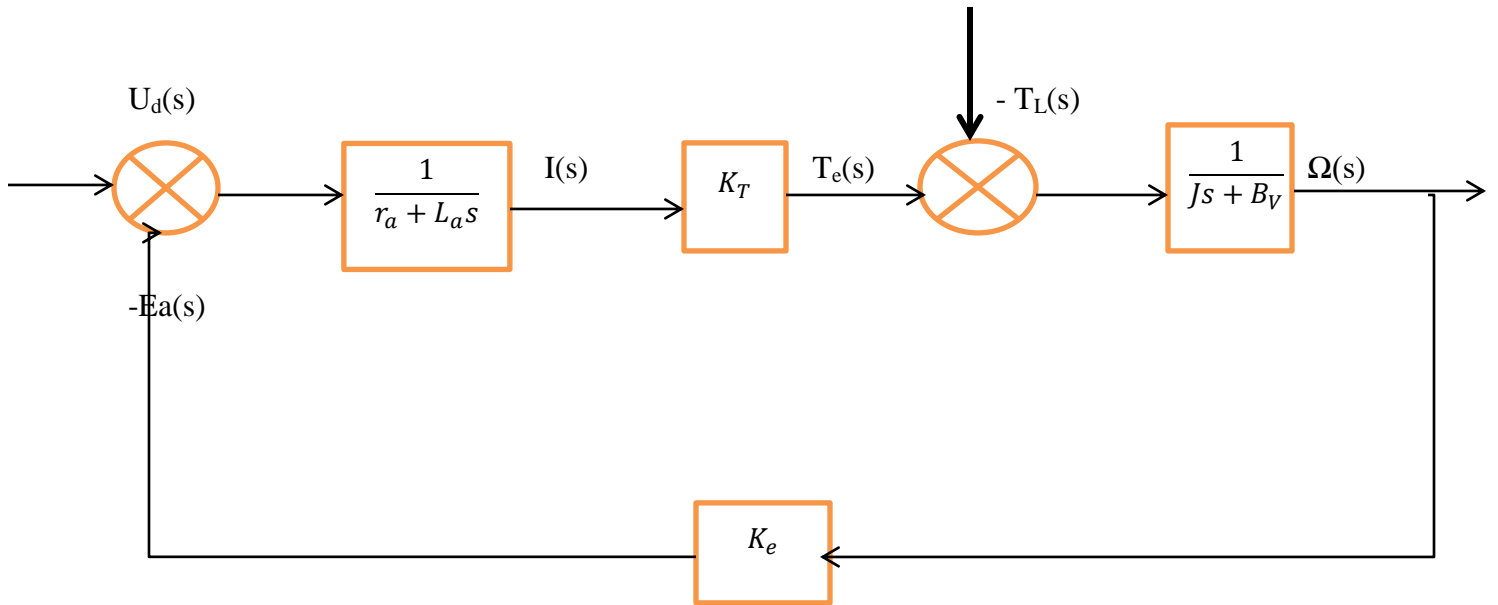


Figure 3.20 Speed step response of brushless dc motors without armature inductances[12]



. Figure3.21 structural diagrams of brushless dc motors under load torques

Hence, the relation between speed and torque load the T/F as given as;

$$G_L(s) = \frac{\Omega(s)}{T_L(s)} = \frac{r_a + L_a s}{L_a J s^2 + (r_a J + L_a B_v) s + (r_a B_v + K_e K_T)} \quad (3.38)$$

So, the effect of load torque and voltages in speed response of a brushless dc motors can be expressed as;

$$\Omega(s) = G_L(s) T_L(s) + G_d(s) U_d(s)$$

Then;

$$\frac{K_T U_d(s)}{L_a J s^2 + (r_a J + L_a B_v) s + (r_a B_v + K_e K_T)} - \frac{(r_a + L_a s) T_L(s)}{L_a J s^2 + (r_a J + L_a B_v) s + (r_a B_v + K_e K_T)} = \Omega(s) \quad 3.39$$

3.2.3 State space Equation (SSE)

Contemporary control theory, represents the behavior of a control systems in the form of its state equations. One of the most significant tools of the modern control analysis is the so-called state-space approaches. With the application of the state equations, it is possible to calculate all the independents variable. so that, the entire characterization of the state of the systems can be obtained at any particular time. The state-space approach represent systems behavior by a collection of 1st-order differential equation in terms of states variable.

The state-space approach has become of considerable importance due to the rapid advancement of computer technology to apply a number of different control algorithms and to design control

systems. During the past year, computer-based real-time control strategies including dynamic system identifications, self –adaptive filtering and optimal controls have found extensively used in motor control systems.

All these sophisticated methods of control are essentially relay on the state equations. In the case of a brushless dc motors the state equation may be derived as a result of algebraic transformations of the system differential equations. The initial phase is the proper choice of the state variable. Even though there can be several sets of state variable, they can only be independents and equal in number to the order of the system. The number of state variable in this example are the 3- phases winding angular speed and current of the rotor, and gives a 4th-order state equations written as follows:

$$\dot{Ax} = X \quad 3.40$$

Give example how to write in Microsoft word Where A is the 3*3 matrix $A = A^T$

$$x = [i_A \ i_B \ i_C \ \Omega]^T;$$

$$u = [u_A u_B u_C T_L]^T;$$

$$A = \begin{bmatrix} -\frac{R}{L-M} & 0 & 0 & -\frac{p\psi_{pm}(\theta)}{L-M} \\ 0 & -\frac{R}{L-M} & 0 & -\frac{p\psi_{pm}(\theta - \frac{2\pi}{3})}{L-M} \\ 0 & 0 & -\frac{R}{L-M} & -\frac{p\psi_{pm}(\theta - \frac{4\pi}{3})}{L-M} \\ \frac{p}{J}\psi_{pm}(\theta) & \frac{p}{J}\psi_{pm}(\theta - \frac{2\pi}{3}) & \frac{p}{J}\psi_{pm}(\theta - \frac{4\pi}{3}) & -\frac{B_V}{J} \end{bmatrix}$$

$$B = \begin{bmatrix} \frac{1}{L-M} & 0 & 0 & 0 \\ 0 & \frac{1}{L-M} & 0 & 0 \\ 0 & 0 & \frac{1}{L-M} & 0 \\ 0 & 0 & 0 & \frac{1}{L-M} \end{bmatrix}$$

The angular position of the rotors, which was indicated in Equation (3.40), can be measured with a position sensor. The permanent magnet flux linkages is not affected by speed or currents, and is only a matter of the rotor position Θ , since the armature reaction is ignored. Therefore, Θ considered as a constant number in the equations. But, in the analysis of controllability, it should

be mentioned that Θ changes with time, as the motors rotating and thus Amatrix is time-dependent. As a result, the state equations expressed in Equations(3.40) is a time-variation, continuously valued, MOMI linearize systems. Since the controllability is one of the major dimensions of optimal estimations and controls, it should be assessed. Hence, the controllability matrix's may be defined as follows;

$$[M0 \quad M1 \quad M2 \quad M3] = M \quad (3.41)$$

So matrix M given as,

$$\begin{bmatrix} \lambda & 0 & 0 & 0 \\ 0 & \lambda & 0 & 0 \\ 0 & 0 & \lambda & 0 \\ 0 & 0 & 0 & -\frac{1}{J} \end{bmatrix} \begin{matrix} M1 \\ M2 \\ M3 \end{matrix} = M \quad (3.42)$$

Where $\lambda = \frac{1}{L-M}$

The matrix M is established to have the rank condition M equal to four . Therefore, the systems described by Equations(3.40) is fully controllable, all systems pole to be positioned placed arbitrarily through state feedbacks.

The initial characteristic are the variations curve of currents and speed during the transition from standstill to stable speed under a constant DC bus voltage. At the moment of start-up, electromotive force and speed are both 0, and I_a expressed as -

$$\frac{U_d - \Delta U}{r_a} = I_a \quad (3.43)$$

Δ shows the voltage drops on the switch of the bridge inverter controller. Figure3.23 shows the armature currents and speed characteristics during the start-up process. As indicated, with a relatively small armature windings resistance and voltage drops of the power switch, a large starting currents can be experienced in a short-duration which can be many to greater than the normal operating currents, more than 10-times. This is acceptable and beneficial to rotor acceleration enabling the motors start rapidly even at full loads. For instance, this is that both the initial back-electromotive force and speed are zero at the rated operating point.

In addition, immediately after starting, the armature currents rise very quickly. Therefore, the load torque smaller than electromagnetic torques resulting in a quick increase in the speed. Once again, these cause the back-electromotive force to build, so the armature currents increase more slowly until the maximum arrives. After that, the armature current will begin to reduce. When the electromagnetic torque reduces, the armature current will diminish, slower rate accelerations Eventually, the load and electromagnetic torque will become equal at which time the speed will maintain at a value near the rating speed, this is when the BLDC motor will stabilize or operate in steady-state operation. Assuming that starting current is not limited, the speed curves

developed in fig 3.22 will be dictated by the motor's damping ratio. From the T/F of the motors, when $0 < \xi < 1$, the system is underdamped and the speed and current will stabilize after overshoot and oscillation, and are demonstrated in figure 3.23.

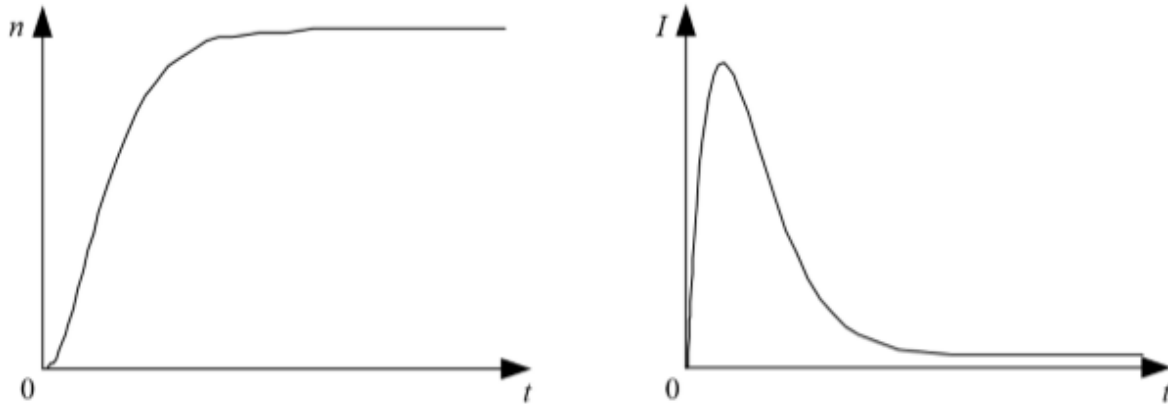


Figure 3.22 curve of currents and speed throughout the motor starting process [12].

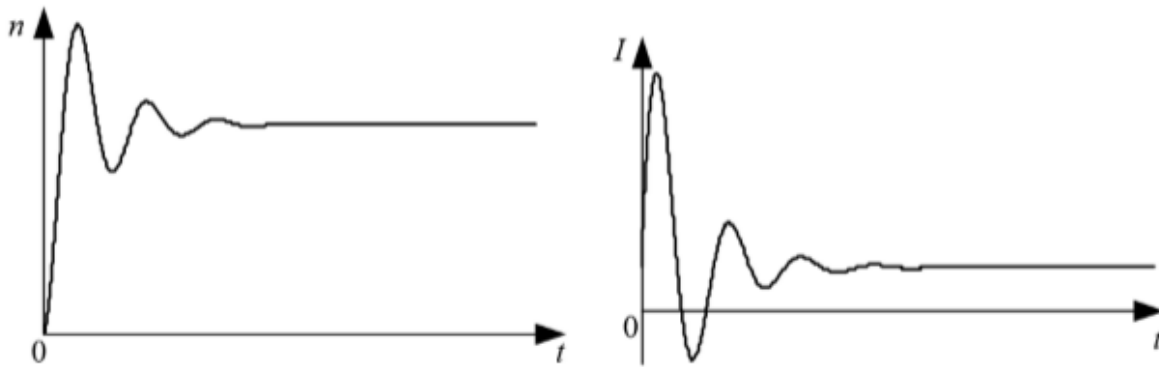


Figure 3.23 oscillation and overshoots during starting process [12].

Power systems The power switch in the drive circuits are very susceptible to overcurrents in power systems, and can fail fast when the current goes beyond their maximum current limit. For instance, IGBT can normally withstand an overcurrent of a duration that is below $10 \mu\text{s}$. Higher-capacity power switches are typically required to switch high inrush currents during startup of a motor that may easily be many times larger than the rated current. Consequently, the current per switch in normal operation is normally much less than its designated value. The result is low efficiency of utilization and high cost because the switches are not fully utilized. During the design process, therefore, the choice of power switch is very important considering the nature of motor starting and performance needs.

There is also a need to control the starting current in a proper way. The increase in current should be rapid enough so that it could achieve fast dynamics response and at the same time keep the power switches safe. The distributions of the magnetic field in the air gap of a BLDC motor is

trapezoidal. Thus, where a phase winding conducts in the trapezoidal portion of the back electromotive force edge, the electromotive force is not very large. This causes the normal starting current lower value than armature current, and can be much higher than a similar DC motor.

3.3.1 Steady-State Operations

3.3.1.1 Operating Characteristic

Operation characteristic indicate how output torque, armature currents armature current and motors efficiency vary with a constants U_d . Based on Equation (3.21), the bigger the load torque, the bigger the armature current to produce the necessary electromagnetic torque to balances the load torque. This will guarantee consistent motor running and the inputs power of the motors can be defined as:

$$P_1 = U_d I = r_a I^2 + \frac{\pi}{30} k_e n I + \Delta U I \quad (3.44)$$

And

$$P_1 = P_{Cu} + P_e + P_T \quad (3.45)$$

Where

n --- the motor speed;

$I^2 r_a = P_{Cu}$;

$k_e n I = P_e$;

$\Delta = P_T$;

The input power given in Equation (3.45) is composed P_T , P_{Cu} and P_e loss bridge power switches, copper loss and electromagnetic power respectively. Which utilized to counteract electromagnetic force, the energy convert into mechanical power during magnetic fields in the rotors then generate electromagnetic torques, considering the load loss then the power transfer as:

$$P_e = (T_L + T_0)\Omega = P_2 + P_0 \quad (3.46)$$

From equation (3.46) P_0 , P_2 , T_0 and T_L represents the no- load loss, power output, no- load torque and load torque respectively. Considering that $T_0 = \frac{P_0}{\Omega}$ and $P_2 = (T_L \Omega)$ the relationship between torque and power can be expressed accordingly.

Efficiency of motor expressed as;

$$\eta = \frac{P_2}{P_1} = \frac{P_1 - (P_{cu} + P_T + P_0)}{P_1} = 1 - \frac{\Sigma P}{P_1} \quad (3.47)$$

So, the equation(3.47) written as:

$$\eta = 1 - \frac{r_a}{U_d} I - \frac{(P_T + P_0)}{U_d I} \quad (3.48)$$

Therefore, the extreme equation (3.48) can be expressed as; since derivative of efficiency is equal to zero.

$$\frac{d\eta}{dI} = -\frac{r_a}{U_d} + \frac{P_T + P_0}{U_d I^2} = 0 \quad (3.49)$$

$$P_T + P_0 = U_d I^2 = P_{cu} \quad (3.50)$$

It is also notable that in Equations(3.50),the Pcu loss varies under the load hence the term of the Pcu loss variable loss conversely, the expression P0+PT is constant irrespective of the load and it is termed as invariable loss. When the invariable loss is equal to the variable loss, the motors will be operating at a maximum efficiency as shown by Equations(3.50). Figure3.24 illustrates the dependence between efficiency and armature currents of the brushless dc motors as the load torque varies, but holding the supply voltage (U d) constant.

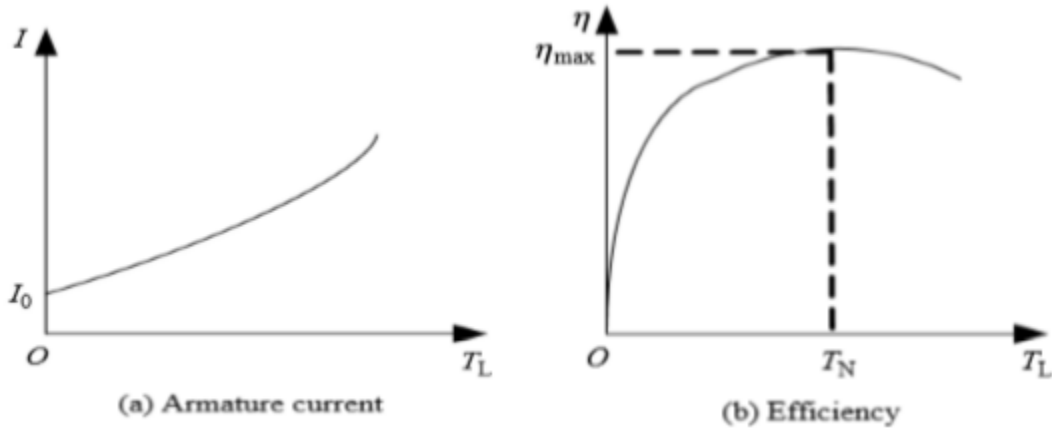


Figure 3.24 curve of efficiency and armature current [12].

3.3.1.2 Regulation Characteristics

The regulation characteristics how the motor describes n varies with U_d when the T_e is kept constants. Under assumption the loss of power switch is ignoring, there exist steady-state conditions in the operation of the motor.

$$U_d = r_a I + \frac{\pi}{30} K_e n \quad (3.51)$$

$$K_T I - T_L = \frac{\pi}{30} B_v n \quad (3.52)$$

Then:-n

$$n = \frac{30K_T}{\pi K_T K_e + \pi r_a B_V} U_d \frac{30r_a}{\pi K_T K_e + \pi r_a B_V} T_L \quad (3.53)$$

Different electromagnetic torques are represented in the $n - U_d$ curves in Figure 24, while $T_{e1} < T_{e2} < T_{e3} < T_{e4}$ are shown in Figure 3.25 these curves reveal the presence of dead zone in characteristic of regulation. Below the dead zone, when the U_d signal changes, it is not enough electromagnetic torque to bridge the load torque and therefore allow the motor to start and remains at $n = 0$. The motor can be start to operate at steady state when the threshold voltages less than U_d .

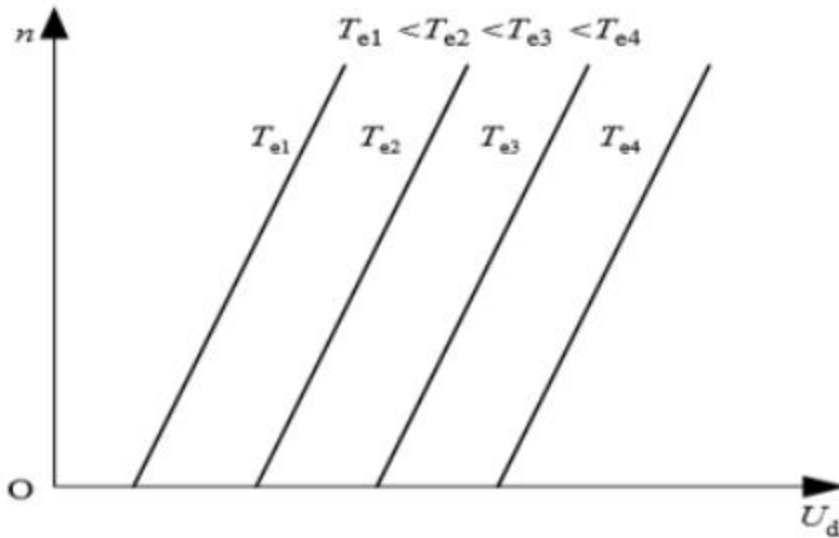


Figure 3.25 the brushless dc motor characteristics of regulation [12].

3.3.1.3 Mechanical Characteristic

Equation (3.51) can be used to determine the relationship between T_e and n at a constant U_d and is represented in the following way:

$$T_e = K_T \frac{30U_d - \pi K_e n}{30r_a} \quad (3.54)$$

Such that;

$$n = \frac{30}{\pi} \frac{K_T U_d - r_a T_e}{30r_a} \quad (3.55)$$

Using Equation (3.55) the characteristic curves of mechanical characteristics of different values of U_d distinctive can be drawn as shown in Figure 3.26. The sequence of the resulting curves is in this figure determined by the relationship $U_{d4} < U_{d3} < U_{d2} < U_{d1}$. In the working model though it is a linear relationship represented by Equation (3.55), in real practice, there is no longer a

strictly linear mechanical characteristic curve because the armature reaction and variable losses lead to loss in the curve.

Figure 3.26 demonstrates that the motors T_e increases and speed (n) declines and an increase in U_d moves the whole curve upwards. As the power electronic switches of brushless dc motor do not have a linear saturation characteristic when commutating, the voltage drops across the switches rises rapidly with armature current, especially when the motors is brought close to the stalled conditions. As a result, the characteristic curves of the mechanism has a sharp negative curve towards its end. Therefore, the speed regulation of a brushless dc motors is mostly achieved through pulse width modulations.

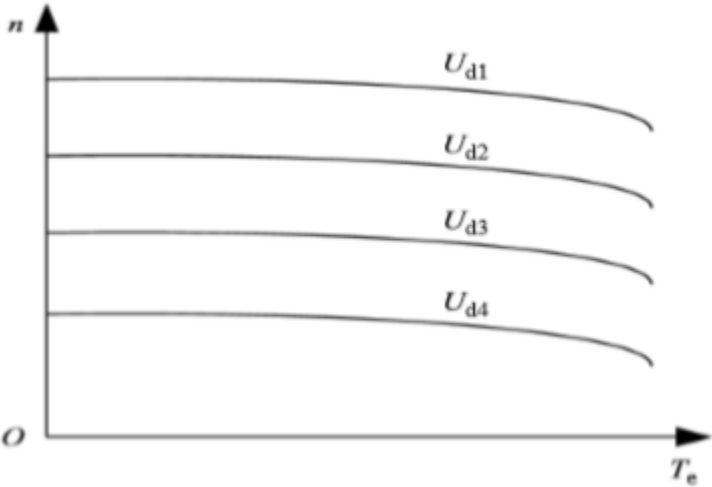


Figure3.26 the brushless dc motors mechanical properties [12].

CHAPTER FOUR

CONTROLLER DESIGN OF BRUSHLESS DC MOTORS

The motor design controllers are designed to operate with brushless dc motor. Brushless dc motor controller design The controller design is built to be compatible with brushless dc motor. Speed control of Brushless dc motor is an important factor in the current motor control systems. There are broadly three control techniques of brushless dc motors namely: open-loops and closed-loops. The most widespread of them is the so-called dual closed-loop speed controls.

The inner loops, in this arrangement, is either the current loop or the torque loop and the outer loop is either the speed loops or the voltage loop. In normal or low-speed mode (of operation, usually lower than the rated speeds) the armature input voltages is varied by the use of Pulse Width Modulations. In high-speed operation surpassing the rated speeds, weakening of the fluxes may be obtained by the progressive movement of the excitation current or the provision of an auxiliary flux to sustain desired operation. Overall, there are a number of methods used in the control of motor speed of brushless dc . This chapters is concerned with the implementation of the dual closed-loops speed controls, intelligent controls strategies and fuzzy logic-based speed control systems of brushless dc motors

4. PID Controller

The Proportional-Integral-Derivative controller is popular with industrial applications because it has a very simple structure and only a small number of adjustable parameter need to be set. The integrals component assists in the removal of steady-state errors. The derivatives component forecasts the behavior of the system and enhances stability.

Proportional-Integral-Derivative parameters are usually tuned on the basis of the step response of the systems. The Proportional-Integral-Derivative controller computes the error ($e(t)$) which is defined as the difference b/n the actual system output and the reference input. The control signal ($U(t)$) is produced as a linear sum of proportion, integration and derivative functions as illustrated below:

$$U(t)=K_P e(t) + K_i \int e(t)dt +K_p de/dt \quad 4.0$$

4.3 Fuzzy Logic Controller is employed in this application.

As shown in fig 4.7, an average fuzzy control systems has two key components which include the fuzzy controls and the plants.

The fuzzy- controls per se is composed of four main elements:

1. Fuzzifications
2. Knowledge bases

3. Fuzzy inferences

4. Defuzzifications

Fuzzy controls is more or less like human reasoning. It is a smart control method which is not based on an accurate mathematical system models. Irrespective of the nature of the plant whether non-linearity or linearity, a well-designed fuzzy control may ensure a robust and adaptive performance with acceptable control outcomes.

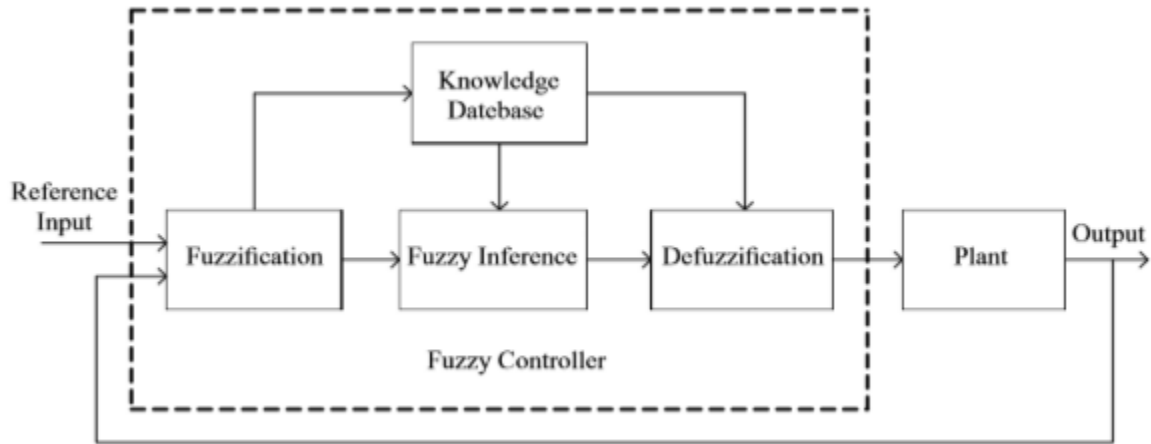


Figure4.1 Schematic diagram of atypical fuzzy control systems [12].

With the advent and advancements of fuzzy theory, fuzzy controls becomes a popular approach in motor-control applications. Due to the large variance of motor loads in many motors application, precise speed-regulations capacity is often critical under all conditions. With reasonable limits on time for computing algorithms, nonlinearity control method such as fuzzy logics are the best options of the motor controls [5-8]. Currently, methods of fuzzy controls to the brushless dc motor can be separated into two principal categorize, optimized fuzzy control and standard fuzzy control

4.3.1 Configuration of FLC

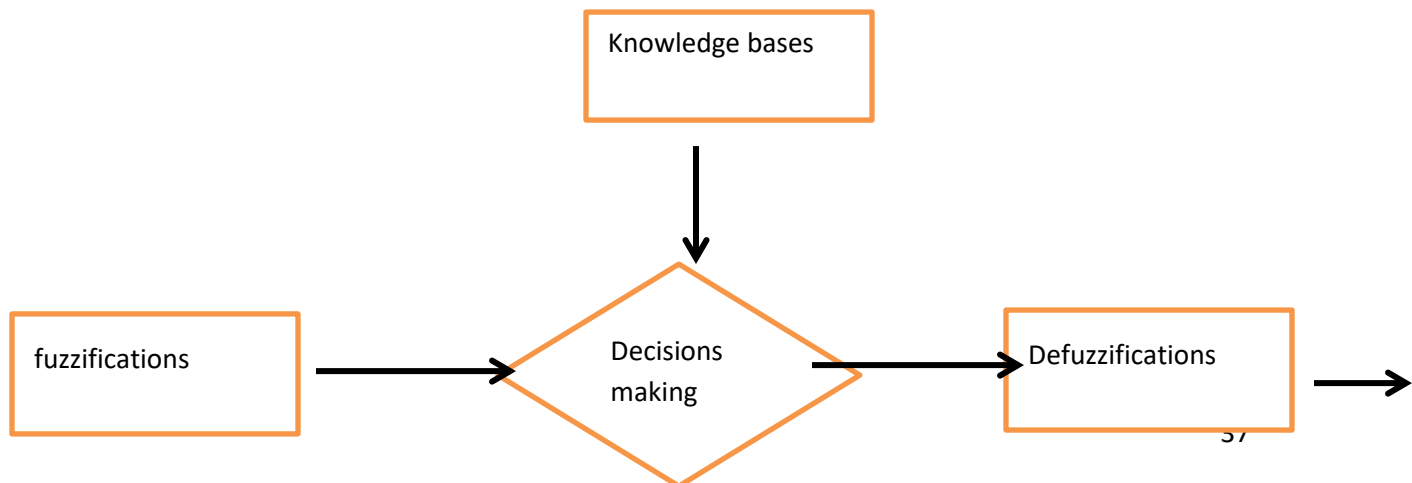


Figure 4.2 Schematic Representation the architecture of a fuzzy control systems

4.3.2 Fuzzifier

As has been mentioned above, fuzzy logics work on the basis of linguistic variables. Nevertheless, as the inputs provided to the Fuzzy Logic Controller are numbers, it would be first necessary to convert the numerical values to linguistic variables- this will be performed by the Fuzzifier. The Fuzzifier converts the crisp input into fuzzy set by allocating them the relevant membership functions.

4.3.3 Knowledge Bases

The fuzzy control system is based on the Knowledge Bases or the Fuzzy Inference Engine. It defines the relationship between output and input fuzzy set, using a set of rule of the type, if, then and fuzzy reasoning processes. This is achieved through this method to obtain a logical output of crisp or fuzzy input. Fuzzy inference systems are available in two main types, the Sugeno and Mamdani types. The most common of these is the Mamdani system which is considered the easiest to use, has wider acceptance, and has been adapted to systems which require human interpretation. The algorithm of the Mamdani (max minimum) inference process is described as follows.

Step 1: determine the degree of fulfillment; by calculating the extent

$$\beta_i = \max [\mu_A(x) \wedge \mu'_A(x)], \quad i = (1, 2, 3, \dots, n) \quad (4.43)$$

Step 2: derived outputs fuzzy set B_i' :

$$\mu_{B_i'}(y) = \beta_i \wedge \mu_{B_i}(y), \quad y \in Y, i = (1, 2, 3, \dots, n) \quad (4.44)$$

Step 3: combine the outputs fuzzy sets B_i' into single aggregated fuzzy sets B' that is:

$$\mu_{B'}(y) = \max \mu_{B_i'}(y), \quad y \in Y, 1 \leq i \leq n \quad (4.45)$$

4.3.4 Decisions making blocks

This is mostly crucial components of a fuzzy control, as it is the blocks which determine the outputs according to the inputs. It generates sensible output applying fuzzy concept and utilizing data, and rule base.

4.3.5 Defuzzifier

Its function is the opposite of the Fuzzifiers. Then, the function of a Defuzzifier is to re-transform the linguistic variables into the crisp ones. There exists a wide variety of Defuzzification techniques.

Although any of the methods can be used, Centroid Defuzzification is most commonly established in fuzzy logic and widely used by researchers in fuzzy logic. It was invented by

Sugeno in 1985 and found higher accuracy results in comparison to others method. The COD process illustrated fig 4.9 and can be represents as follows:

$$\chi^* = \frac{\int \mu_i(x) x dx}{\int \mu_i(x) dx} \quad (4.46)$$

Where:

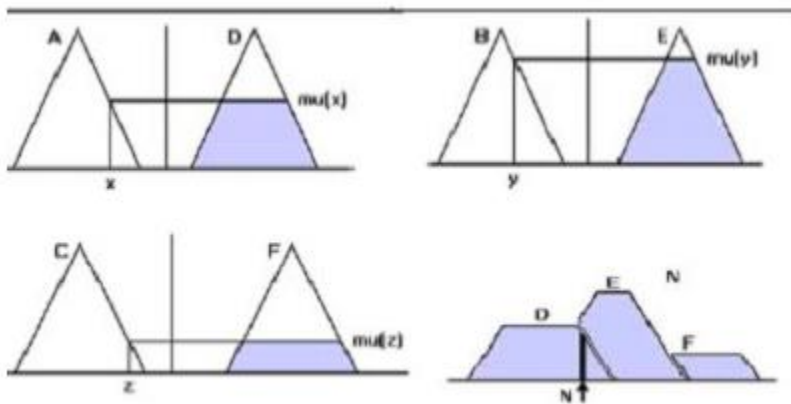
χ^* the defuzzifier output

(x) the aggregating MFs

χ the output variables

Rule 1 if X is A then N is D

Rule 2 if Y is B then N is E



Rule3 if Z is C then N is F

Figure4.3 Schematic Representation of the CoD max-min inferences[12]

4.3.6 Fuzzy Logic based controllers

Continuous monitoring of motor shaft speed is a very important aspect in modern electric drive systems to make sure that it moves in the desired reference direction. A fuzzy logic controller (FLC) can be created to work towards this end. A fuzzy control systems mimics human thought by a rules based designs, which translates linguistic controls expressions into an automated control plan. An important benefit of an FLC is that it offers high control performances ignoring having strict mathematical requirements of the systems.

The development of the fuzzy logic controller is normally done through the following step;

- a. Identification of the systems parameter:

The identification of the systems parameter is conducted by identifying the variables in the construction of the system. Determine the system dynamics parameter that will be used as inputs and outputs to the fuzzy controller. The rotor speed and acceleration are normally selected as input variables and the control output are voltages and frequency.

b. Various Fuzzy- Linguistic Variable are to be selected:

Establish appropriate linguistic terminology and MFs of an inputs and an outputs variable. These fuzzy linguistic variable are used to convert numerical amounts to qualitative (fuzzy) descriptions.

c. Development of the fuzzy controller rule that connects the inputs variable to the outputs variable, of the fuzzy controller, using (if-then) to express the fuzzy logic rules.

d. A fuzzy centroid is used to find the final result of the fuzzy control output.

4.3.7Speed control using fuzzy logic controller

The Fuzzy Logic Controller in motor speed regulation cases normally takes two important inputs variable which are the E as well as the change in CE which is the rate of change in the speed error. In this case, the outputs of the controller is the change in frequency (CF) of the voltages supply to the motor. The following mathematical expression defines these two input variables as follow as;

$$E = V_{ref} - V_{act} \tag{4.47}$$

$$CE = \frac{dE}{dt} \tag{4.48}$$

Where; E =speed error, and CE = change speed error

V_{ref} =the reference motor speed as well as V_{act} = actual measure motor speed.

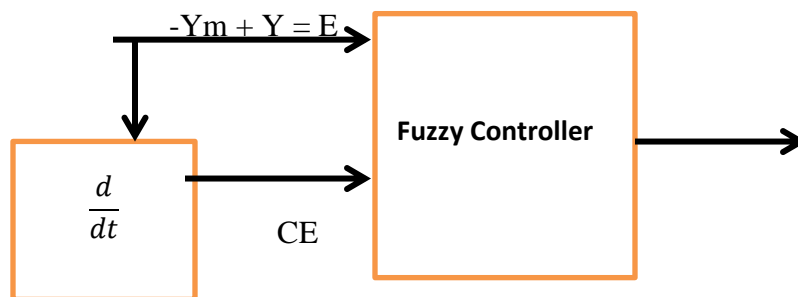


Figure4.4 Schematic Representation of fuzzy control systems.

To create the fuzzy controller, it is feasible to partition every one of the 2- input fuzzy variable into 3- regions, and perform the same partition to the output variables. These areas can be characterized as -ve, zero and +ve. These areas are used to decode the conditions of the control

in the input sides E and CE and to get the adjustment in the frequency in the output side. This frequency change is used to make sure that the speed of the motors is kept close to the desired reference trajectory.

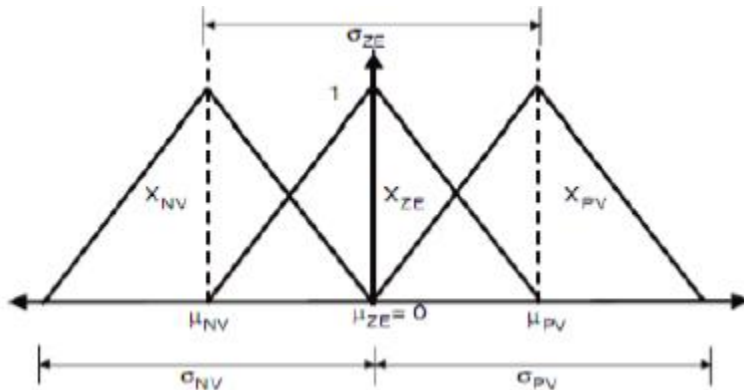


Figure 4.5 An Example of triangular-shaped MFs [12]

+VE and -VE region are typically broken down into smaller sub region, like (PB) and (NM). More often than not, fuzzy logic applications divide a region using an odd number of membership functions, frequently 5 or 7.

4.3.8 Design methodology of fuzzy logic inferences systems using MATLAB Toolbox

The step for designing a FLC in a blank Matlab M -File editor windows are outlined below:

- ✓ Choose input variables for FLC
- ✓ Identify suitable MFs for both input/output variables
- ✓ Fuzzify input variables
- ✓ Design a Fuzzy rule bases for the controller
- ✓ Identify appropriate Defuzzifications method
- ✓ Defuzzify output to provide to a systems for operations.

4.3.9 Select and design MFs

A. the speed errors

Fuzzy-sets	The interval of Membership function	MFs chosen
NL(Negative large)	[-13.35 0 13.35]	Trapezoidal
NM(Medium Negative)	[0 13.35 26.65]	Triangular

NS (Small Negative)	[13.35 26.65 40]	Triangular
ZE (Zero)	[26.65 40 53.31]	Triangular
PS (Small Positive)	[40 53.31 66.65]	Triangular
PM (Medium Positive)	[53.31 66.65 80]	Triangular
PL(Large Positive)	[66.65 80 93.52]	Trapezoidal

Table 4.1 Membership function and fuzzy set of input speed errors.

B. the change speed errors (CE).

Fuzzy-sets	The interval of membership functions	MFs chosen
NL(Negative large)	[-13.35 0 13.5]	Trapezoidal
NM(Medium Negative)	[0 13.35 26.66]	Triangular
NS(Small Negative)	[13.35 26.66 40]	Triangular
ZE(Zero)	[26.66 40 53.33]	Triangular
PS(Small Positive)	[40 53.33 66.67]	Triangular
PM(Medium Positive)	[53.33 66.67 80]	Triangular
PL (Large Positive)	[66.93 80.16 93.6]	Trapezoidal

Table 4.2 Membership function and fuzzy set of change input speed errors.

4.3.10 Designing membership function for CF

Fuzzy- sets	The interval of membership function	MFs chosen

NL (Large Negative)	[-249.8 0 249.8]	Trapezoidal
NM(Negative Medium)	[0 249.8 499.5]	Triangular
NS(Negative Small)	[249.8 499.5 749.5]	Triangular
ZE(Zero)	[499.5 749.5 998.9]	Triangular
PS (positive Small)	[749.5 998.9 1249]	Triangular
PM (medium positive)	[1003 1253 1503]	Triangular
PL (Large positive)	[1249 1499 1750]	Trapezodal

Table 4.3 Membership function and fuzzy set of change output controls.

4.3.11 Fuzzy Rule Bases

In the proposed fuzzy control systems, there are seven fuzzy sets of the variable of speed errors and seven of the change of speed errors variable hence the total of forty nine rule that guide the process of making decisions. The rule base design is an important process in the design of a fuzzy system because it defines the overall behavior of the system by a collection of fuzzy if-then rule. The proposed controller has a rule bases that is introduced in table 4.4. The highest row in this table is the fuzzy set of the error variables (E), the left column is the change in error variables (CE), and the rest of the table is the resulting control output variables (U).

E	N L	NM	NS	Z	PS	PM	P L
CE							
NL	NL	NM	NL	N M	NM	NM	Z
N M	NL	NL	NM	NM	N S	Z	PM
NS	N L	N M	N M	NS	Z	PS	P M
Z	NM	NM	NS	Z	PS	PM	PL
P S	N M	N S	Z	P S	P M	P M	P M
P M	N S	Z	P S	P S	PM	P M	P M
P L	Z	P S	P S	PM	P M	PL	P L

Table 4.4 Rules base table

In MATLAB, the steps to perform simulation the fuzzy controllers is as follows:

- ✚ Initial , the rule must be made and saved in an M-files with an extensions of .FIS.
 - ✚ Next, open FIS editor by typing fuzzy in matlab command window.
 - ✚ Then, imported desired FIS-file through browsing and selecting with command window.
 - ✚ finally, the FIS file is accessed the fuzzy controller will be ready to be operated.
- The all above will be illustrated in the below figure.

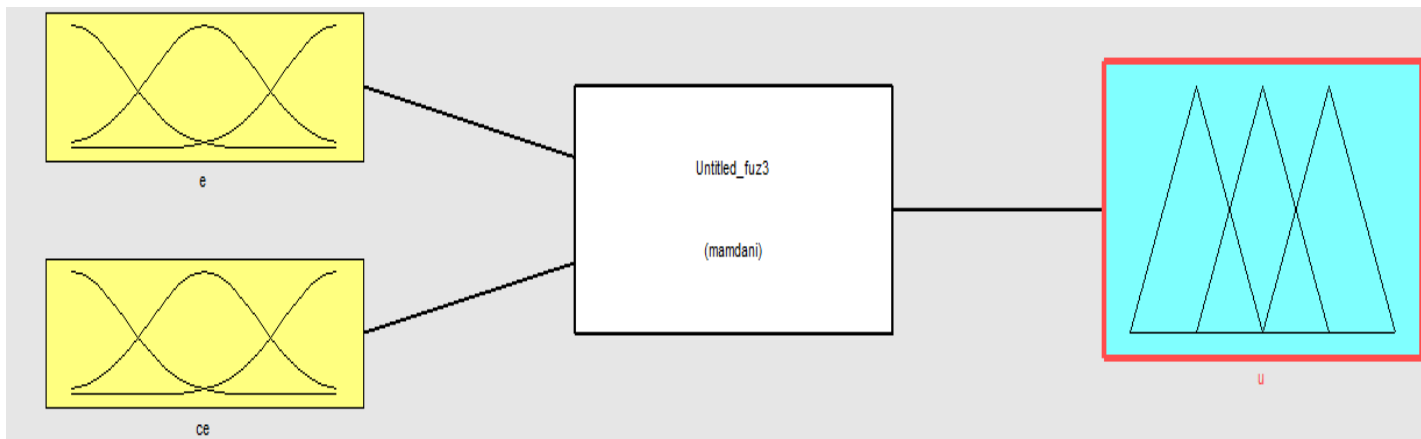
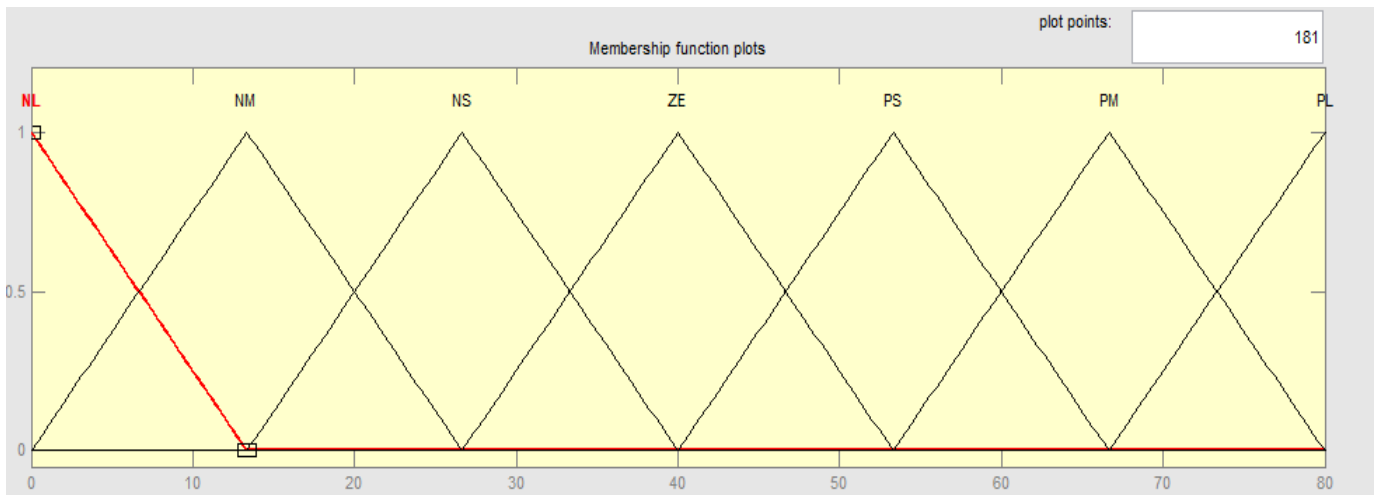


Figure 4.6 FIS Editor Window.



. Figure4.7 MFS of change and input errors

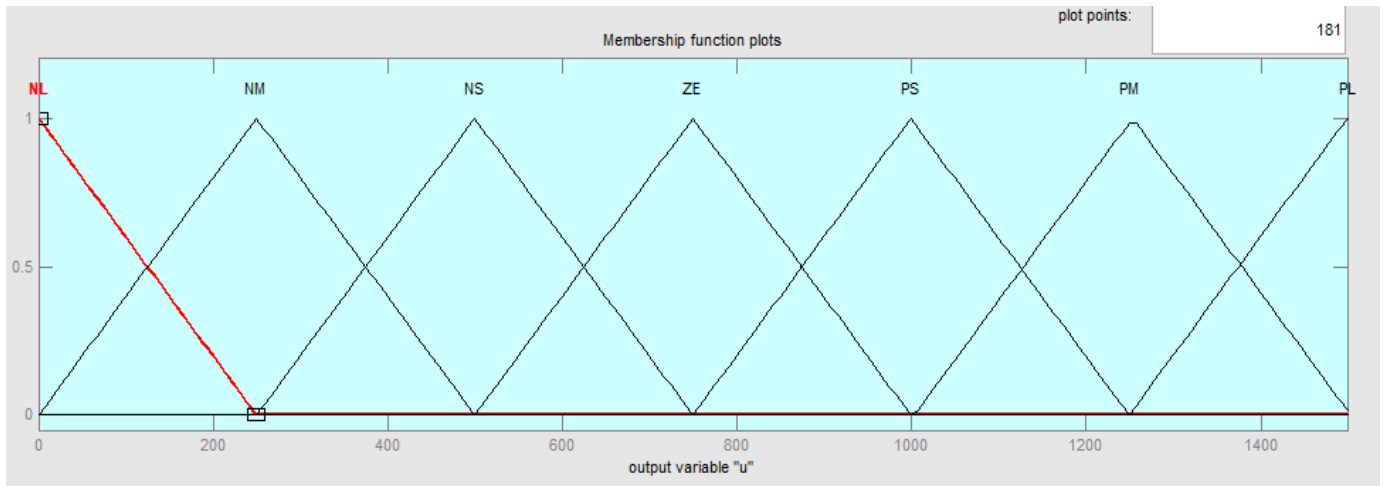


Figure4.8 MFs output changes.

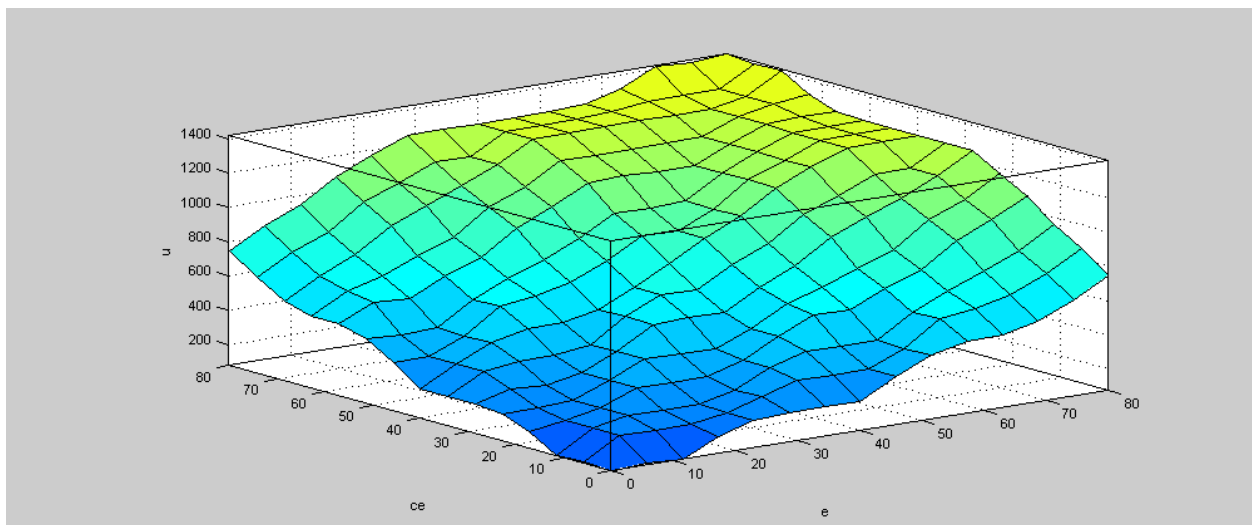


Fig4.9 three- dimensionally image of control surfaces.

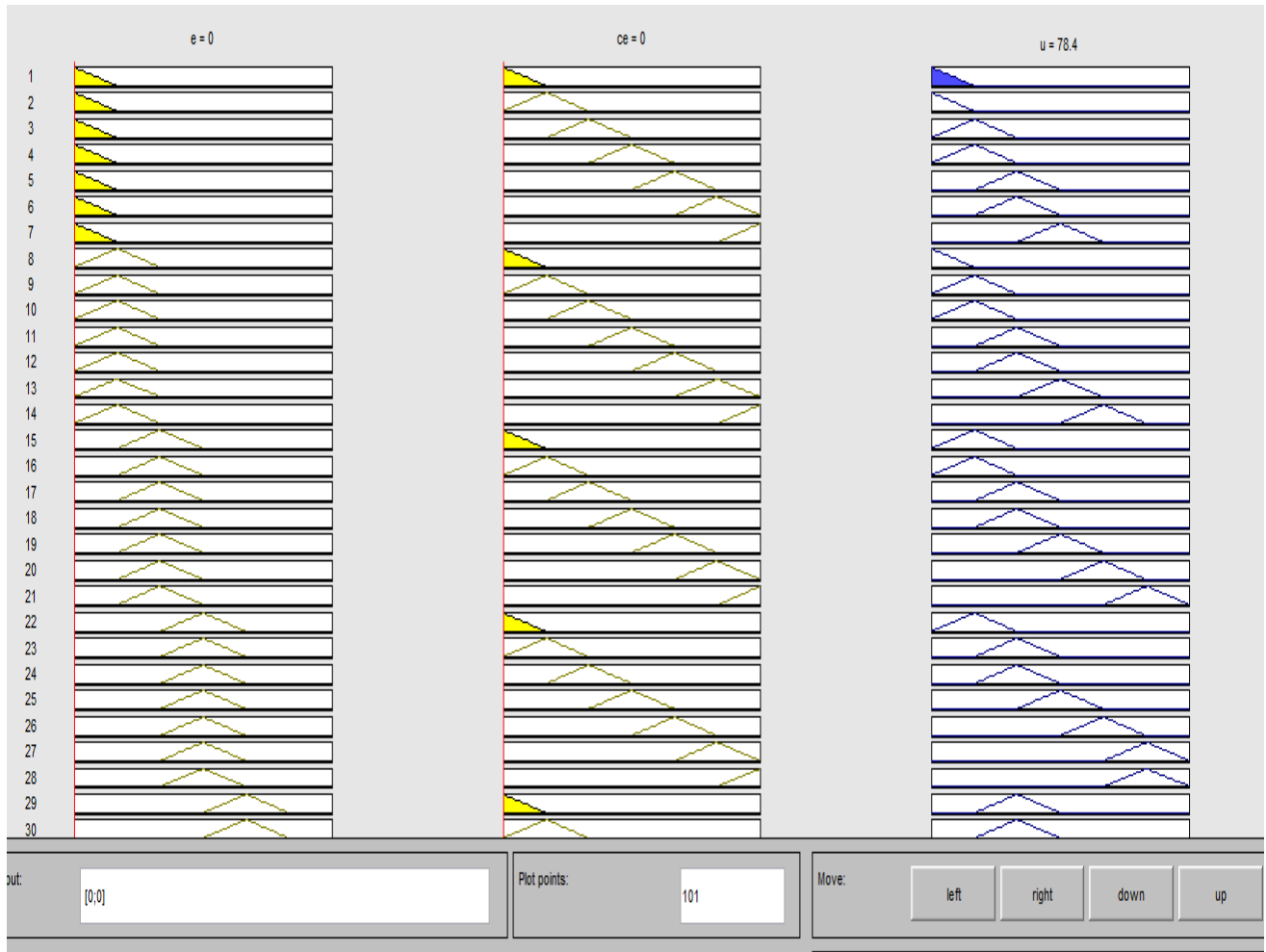


Figure 4.10 Rules Viewer with inputs error, change error and along output (U).

4.4 proposed controller design

Figure 4.11 is a schematic of the proposed design of the motor driving systems of the brush dc motors. This system consists of brushless dc motors, inverters, controller and 3- Hall Effects sensor. As an inputs signal, the references of speed is fed into the controller, and it specifies the desired motor speed. 3-Hall Effects sensor are used to determine the rotor positions and both the controller and actual motors speed are fed with the information. The controller then produces a control signals utilizing fuzzy controls law in order to provide an accurate speed control and system flexibility. This means that this control technique transfers the principles of fuzzy system to nonlinear systems, and the fuzzy control strategy that has been developed in this thesis combines the knowledge of experts operation and the adaptive learning features.

4.4.2 Dynamic BLDC motor specification

Parameters	values
Rated Power	600W
voltage	313V
current	21A
Rated speed	1500rpm
Torque	30Nm
resistance of stator	.44 Ω
inductance of stator	.0025H
constants of inertial	.011
Viscous friction coefficients	.05

Table 4.6 BLDC motor specification [10].

CHAPTER FIVE

RESULTS AND DISCUSSION

The brushless dc motors drive systems was developed and represented in models. All simulations were conducted in MATLAB/Simulink. The input was a step input used as the references signal analyze the control behavior under sudden loads variation .

5.1 Responses of system with PID controller

Figure 5.1 illustrates the proportional-integral derivative controls response of the plants, using Simulink models and with the plants without load response.

Thus, from this Simulink model we have analyzed the system response under PID control while at no load and the rated speed is 1000rpm is supplied for evaluation.

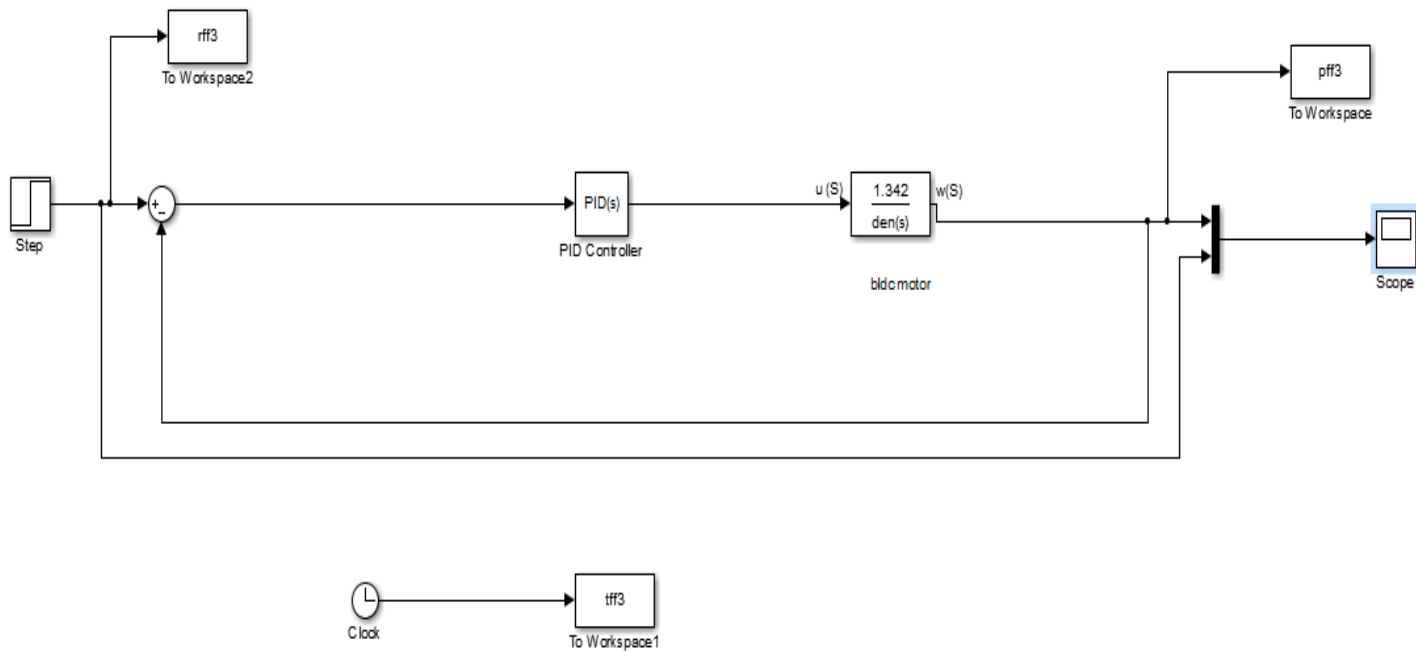
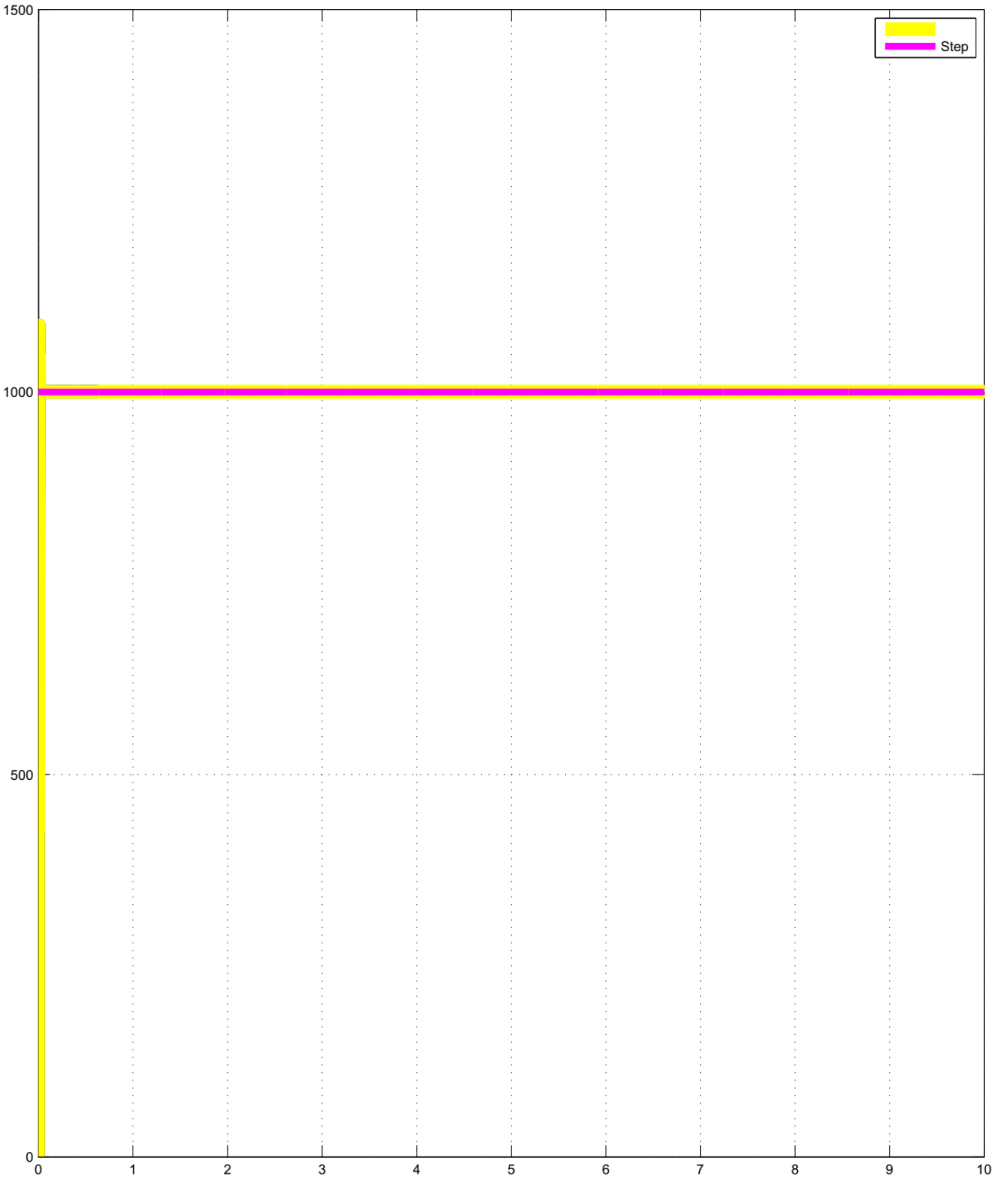


Figure 5.1 Simulink models schematic of the PIDcontrol systems for the brushless dc motors



Time offset: 0

Figure 5.2 Steps responses of the systems with no loads under PID control at 1000 rpm (speed vs time)

N.B :the response graph the yellow color indicate that PID response and the pink color indicate reference input(desire speed).

In Figure 5.2, it is observed that the plants exhibits the rise time of 2.78ms, settling time of 14.782ms and overshoots 16.68% to run this system. Based on the system's response, we noted that it rises sluggishly and its percentage overshoot is unacceptable.

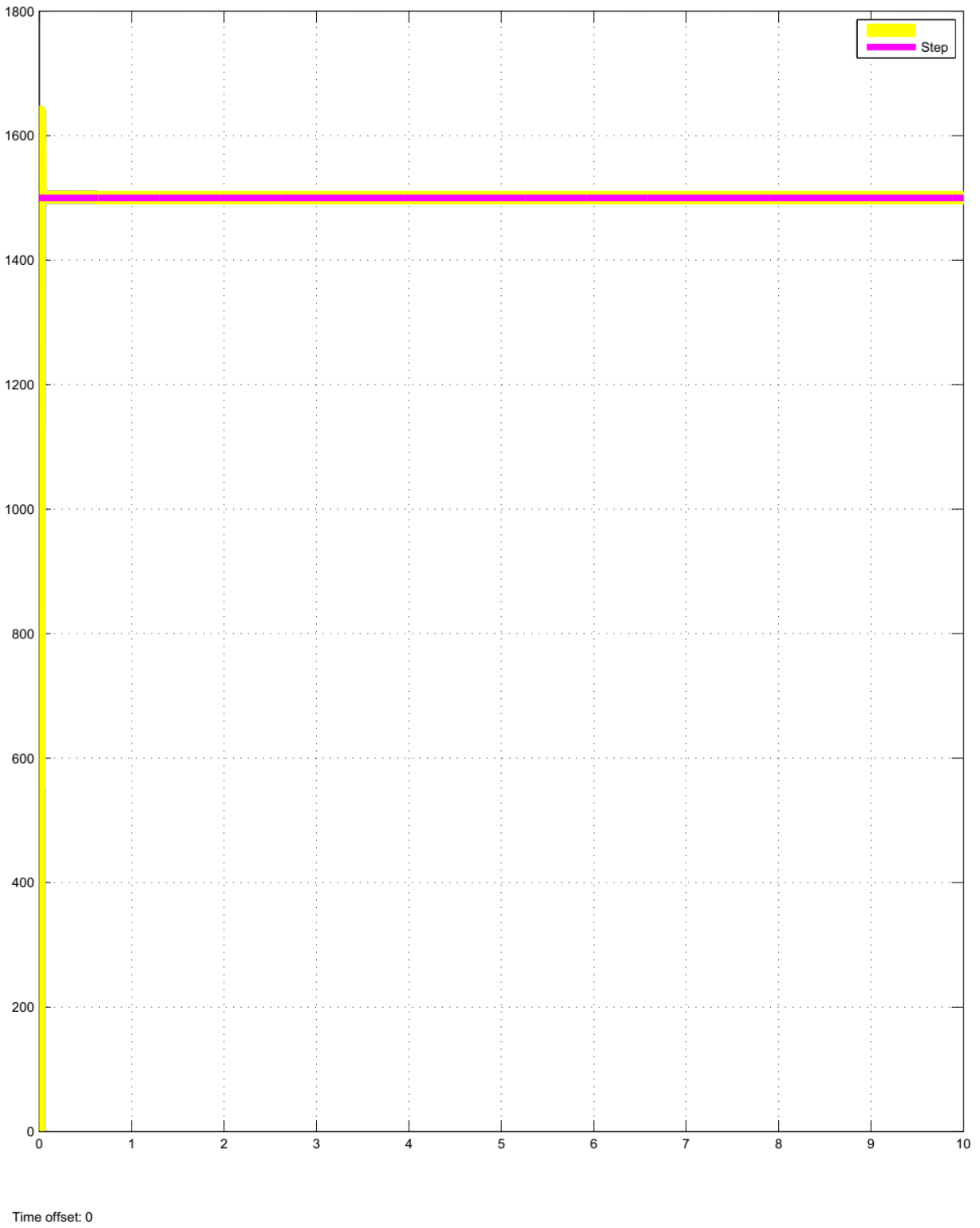


Fig5.3step responses of the systems with no load under PID control at 1500 rpm (speed vs time).

N.B :the response graph the yellow color indicate that PID response and the pink color indicate reference input(desire speed).

We have determined this system's consistent the settling time of increasing from 14.96ms and rise time of 2.78ms and also an increase in percentage overshoot from 17.84 percent with increasing reference input. This can be improved by applying fuzzy logic controller on the system.

5.2 Response of the system with PID controller under load.

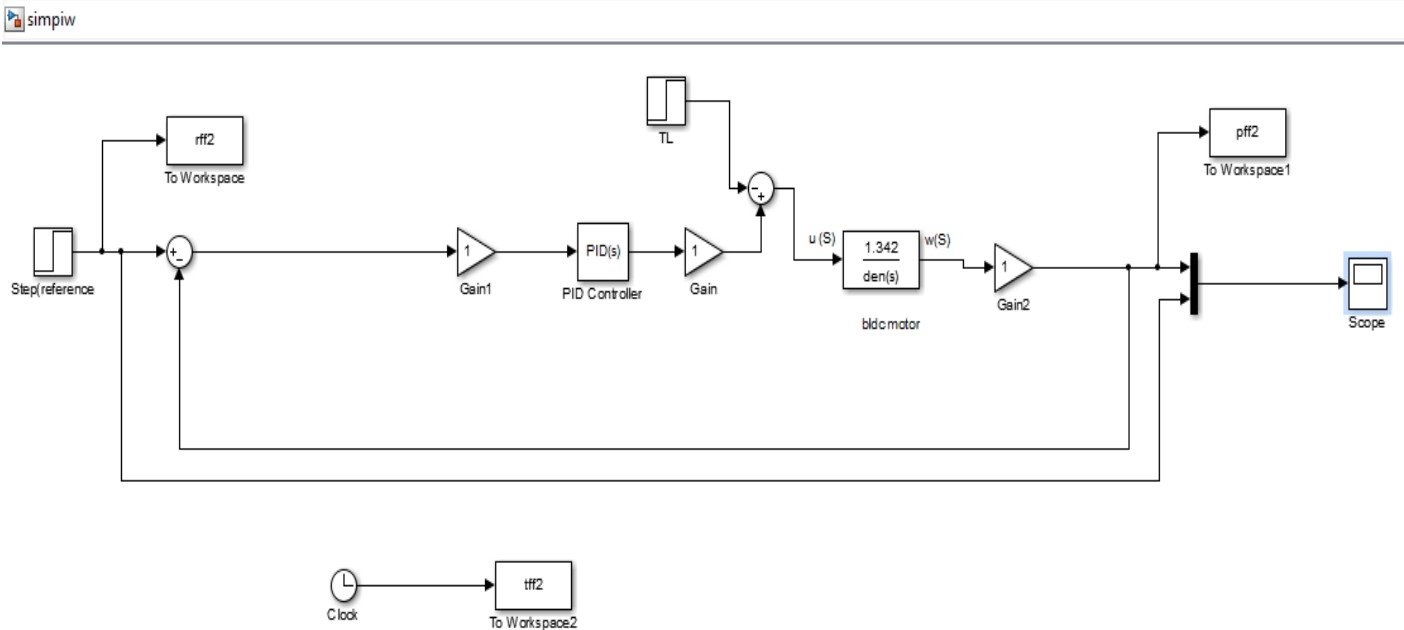
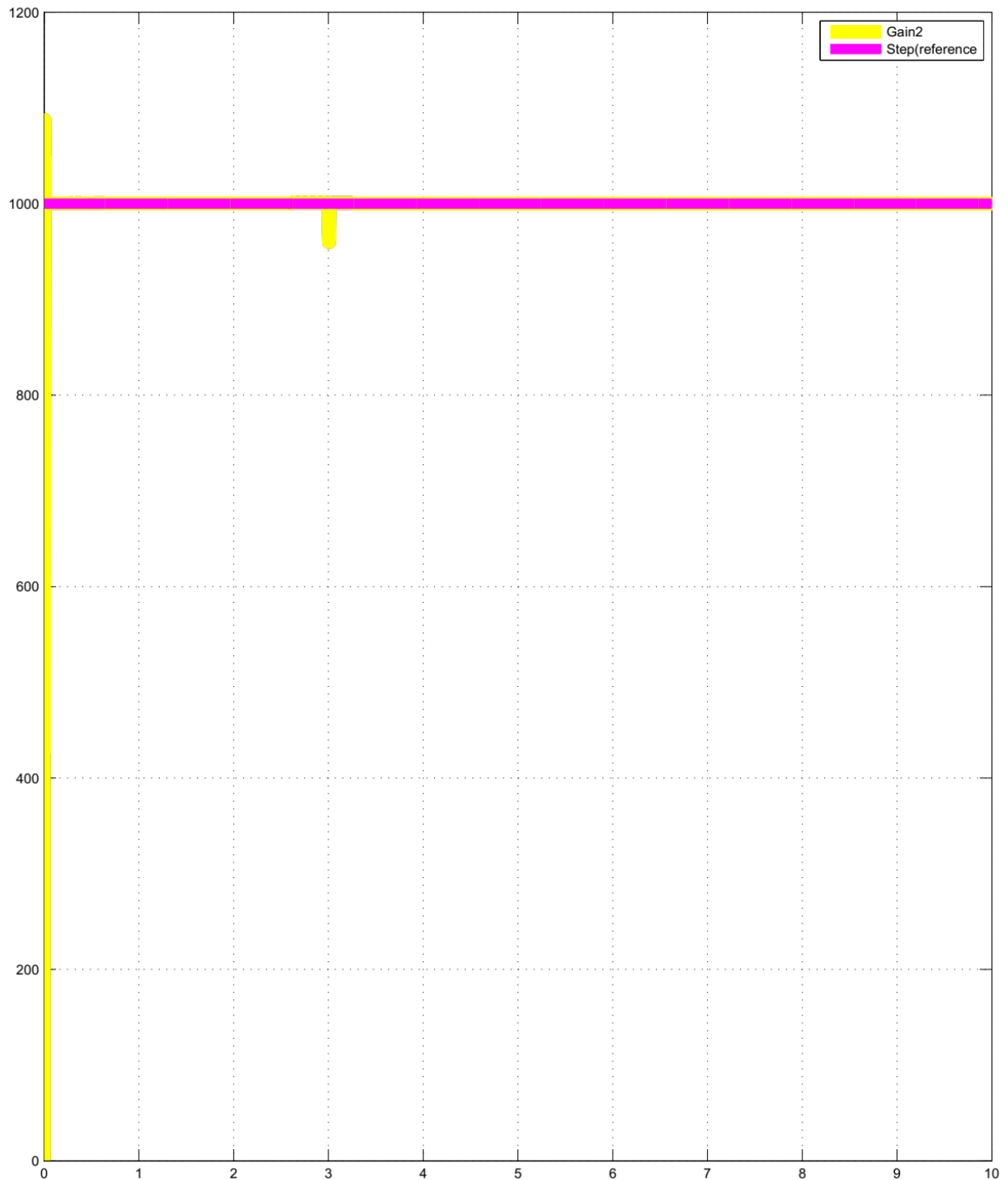


Figure 5.4 Matlab/Simulink model of system with PID control under load.



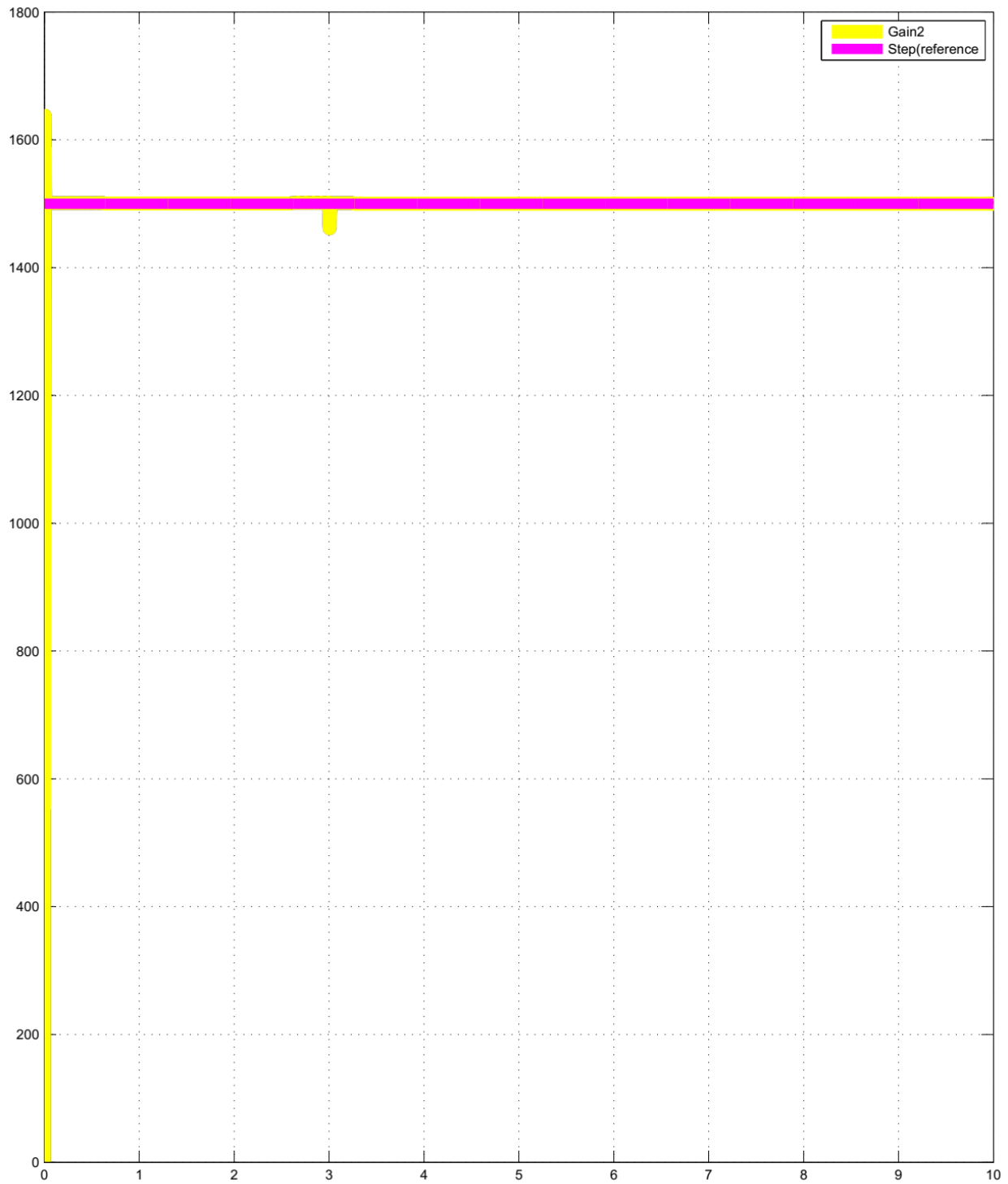
Time offset: 0

fig 5.5 step responses of the systems with PID control under load at 1000 rpm.

N.B :the response graph the yellow color indicate that PID response and the pink color indicate reference input(desire speed).

We can see that the system has a sudden change in load torque, and also the speed will change at 3 sec. plants responded the rise time 2.78ms,settling time 14.782ms and overshoots percent16.68% When 30Nm a load torques was added to system the speeds response starts decrease, it reached the minimum amplitude at 3 seconds, it increased and came back to the speed references.

Figure5.5 and 5.6, the steps response of the proportional-integral derivative control have been shown motor of speed varying (1000 - 1500rpm) with the load torque shown is the rated value of 30Nm. As the controller needs to maintain the steady -state of operating conditions for the plant, we observed that, there is high overshoot in the response (1000-2200 rpm) for 0-3s. Below, a controller with fuzzy technique is designed to reduce overshoot.



Time offset: 0

Fig 5.6 step responses of the systems with load under PIDcontrol at 1500rpm.

N.B :the response graph the yellow color indicate that PID response and the pink color indicate reference input(desire speed).

We have witnessed that this system has constant Rise time of 2.78ms,and some increasing Settling time of 14.96 ms having an increasing percentage of overshoot 17.84 % due to increased reference input. When 30Nm load torques applies to the system, the speeds response of the system started decreasing and it is minimum amplitude 3 second. it goes back to reference speed. we can improve it if we applies fuzzy logic controller on the system.

5.3 System Response no load under Fuzzy Controller

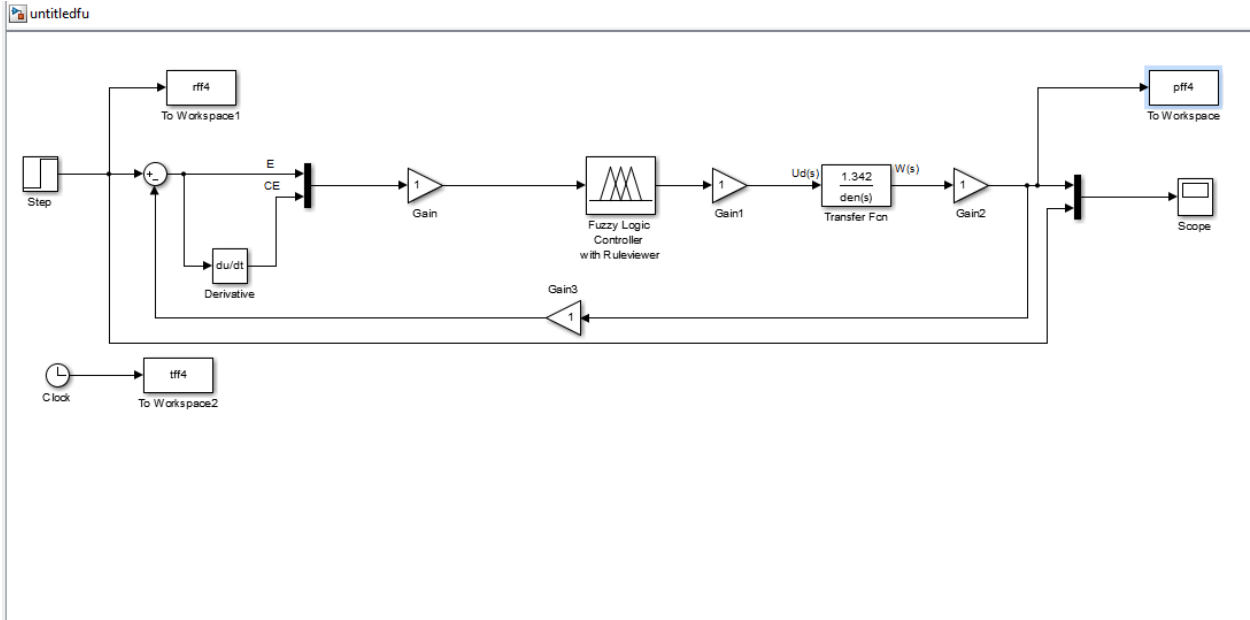
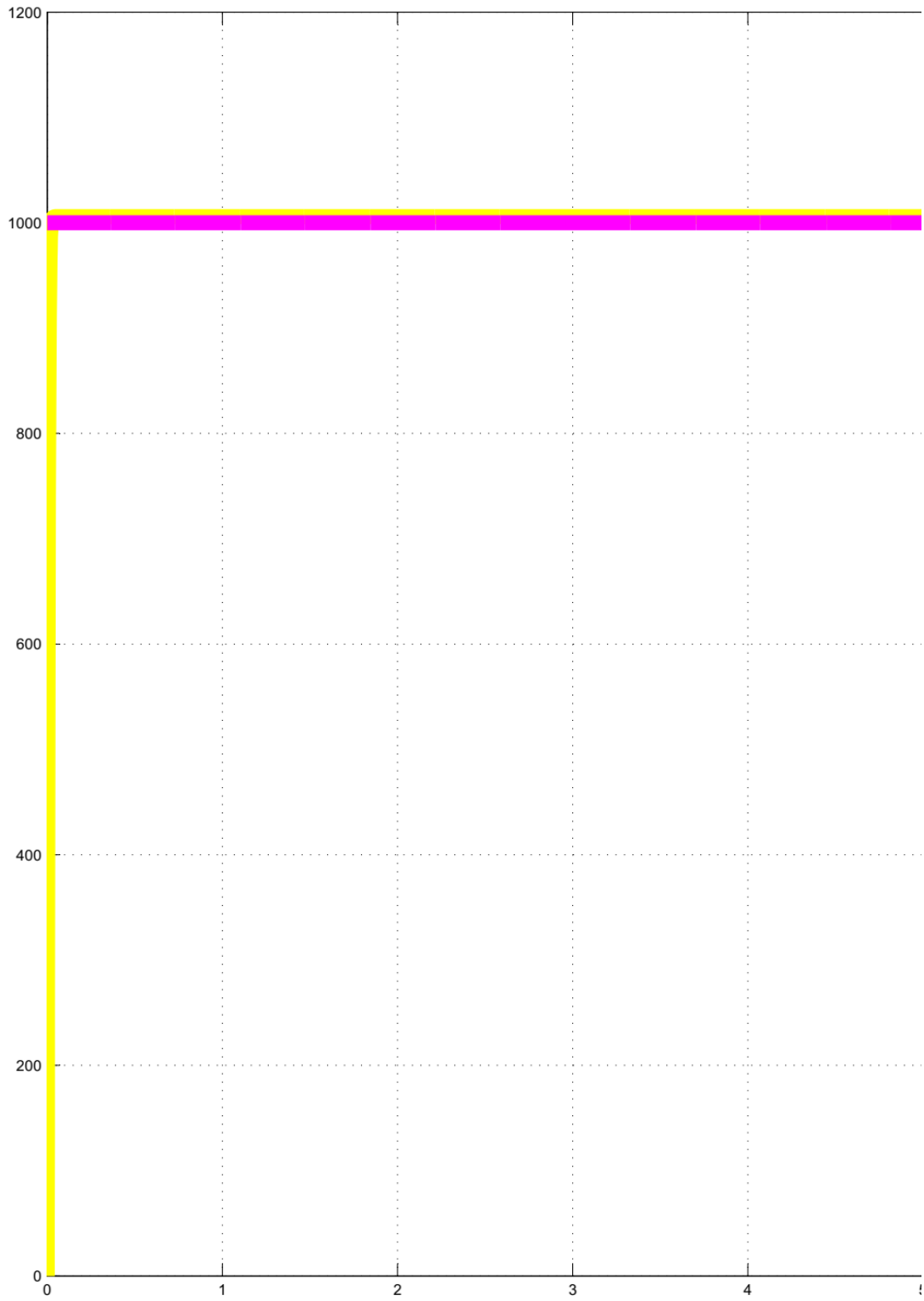


Figure5.7 MATLAB/Simulink model of systems no load under fuzzy controller.



Time offset: 0

Figure 5.8 step responses of the systems no load under fuzzy controller at 1000rpm (speed vs time).

N.B :the response graph the yellow color indicate that Fuzzy response and the pink color indicate reference input(desire speed).

From Figure 5.8, we can see that the plant exhibits a percentage overshoot of 1.654%, settling time 4.125ms and rise time 0.578ms at applied speed 1000rpm. That is from this response of system the understanding and performance of variable very good.

The proposed controller was modeled and tested in Simulink to test the effectiveness of the proposed controller and compare the performances parameters with the PID and the conventional fuzzy controllers. As the figures above show, at no load the simulation outcomes of the proposed fuzzy controllers depict the fact that the system is enhancement in performance at the rated speed. The parameters that are set in the fuzzy controller are meant to provide proper tracking and stability in the systems as opposed to the PID controller response which is poor.

5.3 System Responses with fuzzy controller under load

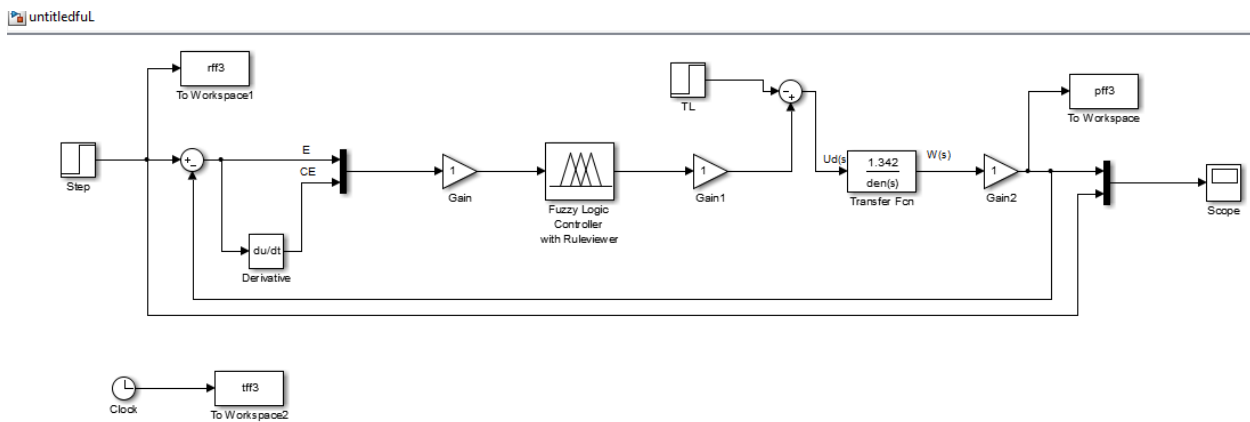
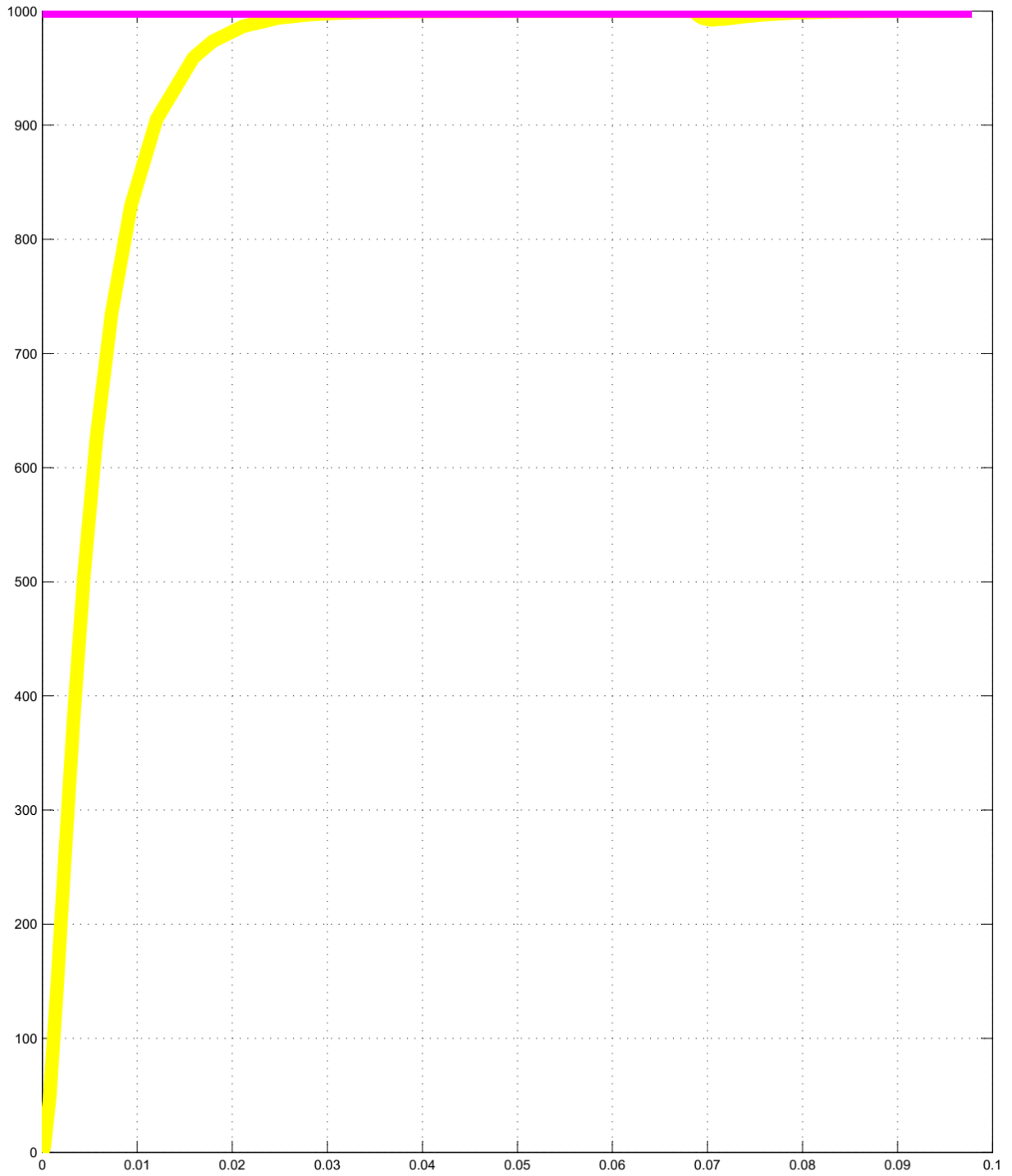


Figure 5.9 MATLAB/Simulink model of system with fuzzy control under load.

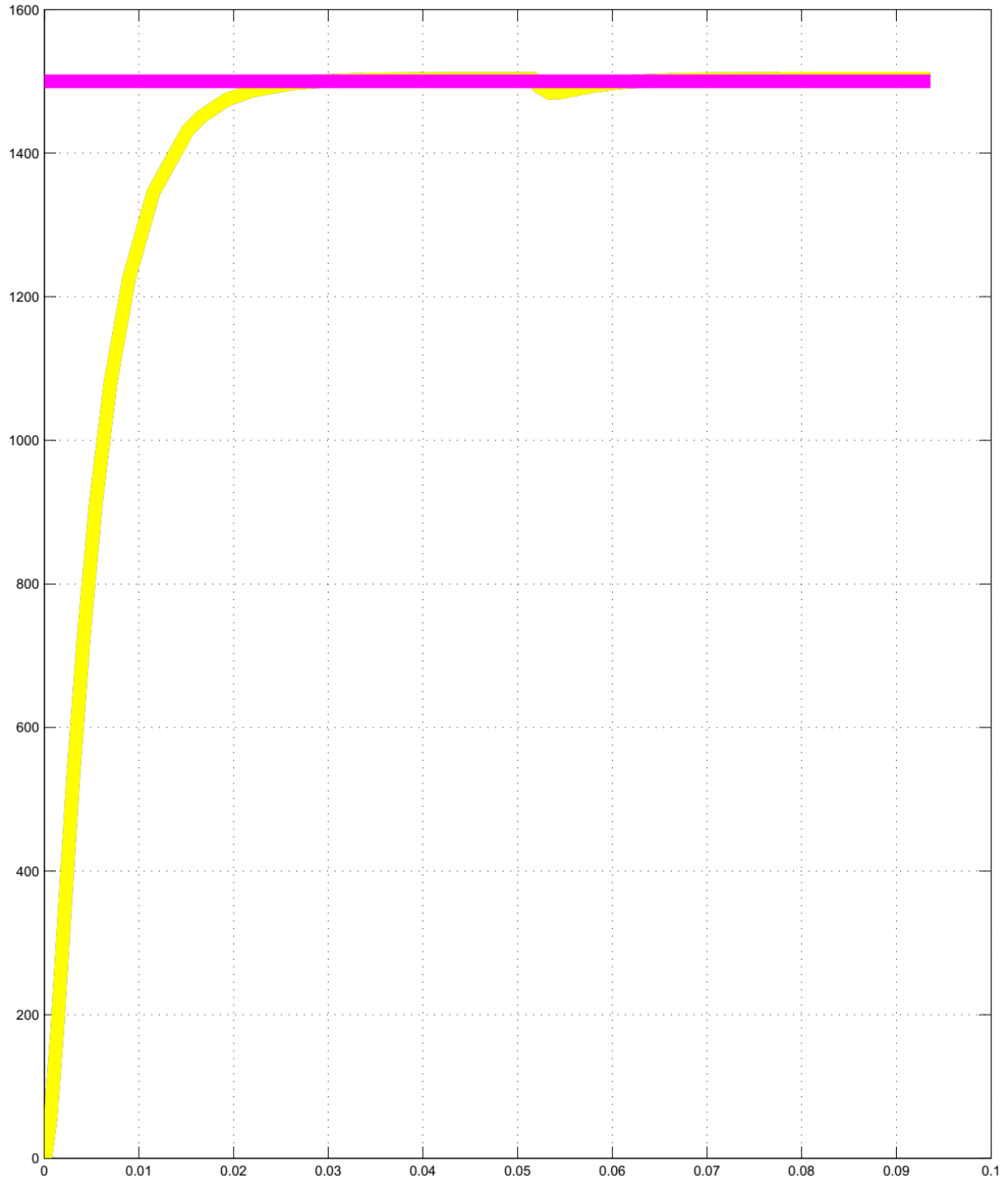


Time offset: 0

fig 5.10 step response of the systems with fuzzy control under load at 1000rpm (speed vs time).

N.B :the response graph the yellow color indicate that Fuzzy response and the pink color indicate reference input(desire speed).

Based on the observation from figure 5.10, the system increasing settling time 3.65ms, rise time 0.685ms and maximum % overshoot 0.684%, at 30Nm load torques applied to the system the speed response of the system will be decreased which its minimum amplitude will be at 0.07 sec then it come back to its reference speed. The rise time represents rapid increases rise time with minimal variation.



Time offset: 0

Fig 5.11 Step response of the systems with fuzzy control under loads at 1500rpm (speed vs time).

N.B :the response graph the yellow color indicate that Fuzzy response and the pink color indicate reference input(desire speed).

From the response graph we observed some considerable change of the close loop -response of the plants using the fuzzy controller relative to the controller is some aspect of performance characteristic. The system exhibit overshoots 0.556%, rise time is 0.625ms and Settling time 3.485ms this indicates that the fuzzy controller effectively suppress the noise and more improve the overshoot compered to PID controller.

Evaluate the effectiveness of the proposed controllers, several test scenarios were conducted, including abrupt loads and speed variation. The result of these tests are shown in Fig5.11. At an operating speed of 1500rpm, the controller was validated with a sudden loads varying that was applied at 0.056s under rated load torques condition.

Response of the system operating at(1000-1500rpm) is present in the fig above. We observe that the fuzzy controllers significantly reduced overshoot as well as disturbance, resulting in lower steady state error and shorter settling time.

5.3 Numerical Performance Comparison

Controlling speed of bldc motor with Fuzzy Control Method has the best controls and performance when compared to PID control methods. The following table below the Compares of the motor's performances characteristic at its rated speed.

5.3.1 Numerical Comparison under No load at Rated Speed

Table5.1 Comparisons of performance characteristic with no load between the two controller at 1000rpm and 1500rpm.

Performance characteristics	PID controller	Fuzzy controller
Maximum Overshoot (%)	16.68%	1.654%
Rise time (ms)	2.78ms	0.578ms
Settling time (ms)	14.782ms	4.125ms
Stability	Good	Moderate

5.3.1 Numerical Comparison with load change at rated speed of 1500rpm and 1000rpm.

Table 5.2 performance comparison with load changes at rated speed

Performances Characteristics	PID controller	Fuzzy controller
Maximum Overshoot (%)	16.68%	0.684%
Rise time (ms)	2.78ms	0.685ms
Settling time (ms)	14.782ms	3.65ms
Maximum Overshoot (%)	17.84%	0.556%
Rise time (ms)	2.75ms	0.625ms
Settling time (ms)	14.96ms	3.485ms
Stability	Good	Moderate

When comparing numerical performances, it is evident that Fuzzy controllers consistently better performance than PID controllers as shown in the previous Figures and tables data comparison.

Looking at the data thus far in Table 5.1 and 5.2, we can see that the PID controller takes more time to settle, high rising time, and higher overshoot when compared to the Fuzzy controller regardless of the, with load and without load. Therefore, this further suggests under those conditions that the fuzzy controller is a better selection than PID as it has the better or improved performance when looking at the speed output of the motors closer to references speed in case of error.

CHAPTER SIX

CONCLUSION AND FUTURE WORK

6.1 Conclusion

The research primarily clarifies of advantage the speed control of BLDCM using fuzzy controller and to a certain extent it very well highlights the inadequate performance of the PID controller particularly under the higher degree of accuracy condition.

Hence, The fuzzy controller was designed, to mitigate the overshoot and decrease the tracking error to achieve a substantially better response and performance upon more conditions than the PID controller.

The BLDC motor model is designed, considering its dynamic characteristics, and the controller is built to develop fuzzy control and PID control for speed control. The controller is developed and implemented through MATLAB/Simulink software. The performance of the strategy is evaluated using MATLAB simulation. It is less expensive than building a real experimental model, and it gives the most precise properties.

Typically, from the analysis of Tables 5.1 and 5.2, we can see that the proportional-integral derivative control for speed regulation of the brushless dc motors shows high rising time, high overshoot, and higher settling time compared to the fuzzy controller in no load condition and load condition as well. This indicate that the fuzzy controllers is preferred better reference speed tracking performance than PID controllers, particularly minimizing positional errors.

The analysis compares performances of a 3-phases brushless dc motors using FLC and proportional-integral derivative control. Furthermore, the performances of FLC and PID controller is compared based on settling time, rise time, and max –overshoot. Simulation result of both proportional-integral dervetive control and FLC are included.

A comparative study carried out between these two approaches demonstrates that fuzzy-logic based control provides better performance in terms of maximizing overshoot and disturbance reduction while providing significantly lower steady-state errors and settling time. Stability of the systems is guaranteed with controller, we have enhanced the existing systems has been improved accurate overshoots percent and improved numerical analysis, while maintaining a good steady-state response.

Let us conclude by summarizing our expectation of the FLC to perform better than BLDC motor PIDcontrollers in the areas of settling time (T_s), rise time and percent overshoot.

6.2 Future work

This research investigates a BLDC motor's speed control in the MATLAB toolbox to establish that Fuzzy control behave better and offer better performance, stability, and efficiency than PID control. The simulation result of controller will not be good and not advisable to use this approach for real time application or experimental results, so we recommended to implement proposed methodology real time (practical) system or experimental results, while conducting complete analysis about others power quality issue like distortions, voltages imbalance, harmonics and develop flux improvement of motors.

To achieve improved performances and efficient of the brushless dc motors with minimum complexity. In addition, system protection should account for under-voltage and over-voltage conditions, and while the machine is operating, a constant supply of electric power should not have any fluctuation in voltage outside the specified limits.

REFERENCES

- [1] Vinod Kr Singh Patel, A.K.Pandey, “Modeling and Simulation of Brushless DC Motor Using PWM Control Technique”, International Journal of Engineering Research and Applications, Vol. 3, Issue 3, May-Jun 2013, pp.612-620., 2005.
- [2] K. Ang, G. Chong, Y. Li, ‘PID control system analysis, design, and technology’, IEEE Trans. Control System Technology, Volume 13, pp. 559 – 576, 2005.
- [3] Atef Saleh Othman Al-Mashakbeh, “Proportional Integral and Derivative Control of Brushless DC Motor”, European Journal of Scientific Research 26-28 July 2009, vol.35, pg 198-203.
- [4] Manafeddin Namazov, DC motor position control using fuzzy proportional-derivative controllers with different defuzzification methods, Turkish Journal of Fuzzy Systems, Vol.1, No.1, pp. 36-54, 2010.
- [5] “Modeling and Control of Three Phase BLDC Motor using PID with Genetic Algorithm”, UK Sim 13 the International Conference on Modeling and Simulation, pp.189-194, 2011. And Simulation, pp.189-194, 2011.
- [6] Anjali.A.R “Control Of Three Phase BLDC Motor Using Fuzzy Logic Controller” International Journal of Engineering Research &Technology (IJERT), Vol. 2, Issue 7, July 2013.
- [7] R. Kandiban, R. Arulmozhiyal “Design of Adaptive Fuzzy PID Controller for Speed control of BLDC Motor” International Journal of Soft Computing and Engineering ,Volume-2, Issue-1, March 2012.
- [8] J. J. E.Slotine, W. Li, “Composite Adaptive Control of Robot manipulators,” Automatica, Vol. 25, pp. 509-519, 1991.
- [9] Adel A.El-samahy and Mohamed A.Shamseldin, “BLDC motor tracking control using self-tuning fuzzy PID control and model reference adaptive control” Ain Shams university ,Ain Shams Engineering Journal (2018) 9,341-352.
- [10] Thasneem. And Shalu George K.”Speed Control of Brushless DC Motor Using Model Reference Adaptive Control”, International Journal of Advanced Research in Electrical, Electronics and Instrumentation Engineering, Vol. 6, Issue 5, May 2017.
- [11] M. A. Shamseldin, and A. M. A. Ghany, M. A. A. Ghany, “Performance Study of Enhanced Non-Linear PID Control Applied on Brushless DC Motor,” International Journal of Power Electronics and Drive System (IJPEDS), vol. 9, no.2, pp. 536–545, 2018.

[12] John Wiley & Sons Singapore “PERMANENT MAGNET BRUSHLESS DC MOTOR DRIVES AND CONTROLS” First Edition. Chang-liang Xia.pp 26-52, Science Press. Published 2012.

[13] Walter, N. A., Stephen, L. H. (2003) Electric Motor Control. Thomson/Delmar Learning, Australia.

[14] Krause, P. C. (1986) Analysis of Electric Machinery. Kinsport Press Inc., Kinsport Town.

[15] Pillay, P., Krishnan, R. (1989) Modeling, simulation, and analysis of permanent-magnet motor drives, part I: the permanent-magnet synchronous motor drive. IEEE Transactions on Industry Application, 25(2), 265–273.

[16] Gao,J.,D.,Wang,X.H.,Li,F.H.(2005) AC Motor and Its Analysis.(2nd edition) Tsinghua University press, Beijing (Chinese).

[17] I. Press, L. Shafer, G. W. Arnold, and D. Jacobson, analysis of electric machinery and drive systems. 2013.

APPENDIX A

MATLAB programmed

Code rule;

[system]

Name = 'Untitled fuz'

Type = 'mamdani'

Version = 2.0

Num Input = 2

Num output = 1

Num Rules = 49

AndMethod = 'min'

Or Method = 'max'

ImpMethod = 'min'

Agg Method = 'max'

Defuzz Method = 'centroid'

[Input 1]

Name = 'e'

Range = [0 1500]

Num MFs = 7

MF1 = 'NL': 'trimf', [-250 -3.553e-15 250]

MF2='NM': 'trimf', [0 250 500]

MF3='NS': 'trimf', [250 500 750]

MF4='ZE': 'trimf', [500 750 1000]

MF5='PS': 'trimf', [750 1000 1250]

MF6='PM': 'trimf', [1000 1250 1500]

MF7='PL': 'trimf', [1250 1500 1750]

[Input 2]

Name = 'ce'

Range = [0 1500]

Num MFs = 7

MF1 = 'NL' : 'trimf' , [-250 0 250]

MF2 = 'NM': 'trimf', [0 250 499.9]

MF3 = 'NS': 'trimf' , [250 499.9 750]

MF4='ZE': 'trimf', [499.9 750 1000]

MF5='PS': 'trimf', [750 1000 1250]

MF6='PM': 'trimf', [1000 1250 1500]

MF7='PL': 'trimf', [1253.96825396825 1503.96825396825 1754.96825396825]

[Output 1]

Name = 'u'

Range = [0 1500]

Num MFs = 7

MF1 = 'NL': 'trimf' , [-250 0 250]

MF2 = 'NM': 'trimf' , [0 250 499.9]

MF3 = 'NS': 'trimf' , [250 499.9 750]

MF4='ZE': 'trimf', [499.9 750 1000]

MF5='PS': 'trimf', [750 1000 1250]

MF6='PM': 'trimf', [1003.96825396825 1253.96825396825 1503.96825396825]

MF7='PL': 'trimf', [1250 1500 1751]

APPENDIX B

title('Six Unit-Step Responses'); % Super title for the entire figure

% first system

zeta1 = 0; % damping ratio

omega_n1 = 10; % Natural frequency

num7 = [omega_n1^2];

den7 = [1, 2*zeta1*omega_n1, omega_n1^2];

% second system

zeta2 = 0.2; %damping ratio

omega_n2 = 10; % natural frequency

num8 = [omega_n2^2];

den8 = [1, 2*zeta2*omega_n2, omega_n2^2];

%third system

zeta3 = 0.4;

omega_n3 = 10;

num9 = [omega_n3^2];

den9 = [1, 2*zeta3*omega_n3, omega_n3^2];

%fourth system

zeta4 = 0.6;

omega_n4 = 10;

num10 = [omega_n4^2];

den10 = [1, 2*zeta4*omega_n4, omega_n4^2];

%fifth system

zeta5 = 0.8;

omega_n5 = 10;

```

num11 = [omega_n5^2];
den11 = [1, 2*zeta5*omega_n5, omega_n5^2];
%sixth system
zeta6 = 1;
omega_n6 = 10;
num12 = [omega_n6^2];
den12 = [1, 2*zeta6*omega_n6, omega_n6^2];
t = 0:0.130:10;
[d7,x7,t] = step(num7,den7,t);
[d8,x8,t] = step(num8,den8,t);
[d9,x9,t] = step(num9,den9,t);
[d10,x10,t] = step(num10,den10,t);
[d11,x11,t] = step(num11,den11,t);
[d12,x12,t] = step(num12,den12,t);
plot(t,d7,t,d8,t,d9,t,d10,t,d11,t,d12);
text(0.95,1.58,'zeta1 = 0')
text(0.4,1.36,'zeta2 = 0.2')
text(0.4,1.24,'zeta3 = 0.4')
text(0.4,1.13,'zeta4 = 0.6')
text(0.4,0.98,'zeta5 = 0.8')
text(0.3,0.86,'zeta6 = 1')
grid
xlabel('t se')
ylabel('speed outputs of zeta1=0,zeta2=0.2,zeta3=0.4,zeta4=0.6, zeta5=0.8,and zeta6=1')

```